Am J Transl Res 2024;16(10):6072-6096
www.ajtr.org /ISSN:1943-8141/AJTR0157600

Original Article

Dystrobrevin beta is a promising prognostic biomarker and therapeutic target for hepatocellular carcinoma

Jin Sun[1,2,3], Yingnan Li[1,2,3], Beibei Bie[4], Hongwei Tian[1,2,3], Jun Li[1,2,3], Lan Yang[1,2], Zhe Zhou[1,2], Yanhua Mu[1,2,3], Zongfang Li[1,2,3,5]

[1]National and Local Joint Engineering Research Center of Biodiagnostics and Biotherapy, The Second Affiliated Hospital of Xi'an Jiaotong University, Xi'an 710004, Shaanxi, China; [2]Shaanxi Provincial Clinical Research Center for Hepatic and Splenic Diseases, The Second Affiliated Hospital of Xi'an Jiaotong University, Xi'an 710004, Shaanxi, China; [3]Center for Tumour and Immunology, The Precision Medical Institute, Xi'an Jiaotong University, Xi'an 710115, Shaanxi, China; [4]Department of Pharmacy, Medical School, Xi'an Peihua University, Xi'an 710125, Shaanxi, China; [5]Department of Geriatric General Surgery, The Second Affiliated Hospital of Xi'an Jiaotong University, Xi'an 710004, Shaanxi, China

Received May 7, 2024; Accepted September 25, 2024; Epub October 15, 2024; Published October 30, 2024

Abstract: Objectives: Dystrobrevin beta (DTNB) is a constituent of the dystrophin-associated protein complex (DPC). Our previous RNA sequencing (RNA-seq) study revealed that knockdown of the oncogenic long noncoding RNA (lncRNA) HOXD cluster antisense RNA 1 (HOXD-AS1) in hepatocellular carcinoma (HCC) cells could reduce the expression levels of DTNB. However, the association between DTNB and HCC remains uncertain. Methods: The upregulation of DTNB in HCC cell lines and the regulatory effect of HOXD-AS1 on its expression were verified using quantitative real-time PCR (qRT-PCR). The potential clinical significance, biological functions and underlying mechanisms of DTNB in HCC were investigated through bioinformatics analysis. The high expression of DTNB was validated in HCC tissues, and its biological function in HCC was investigated by performing loss-of-function assays *in vitro*. Results: DTNB was highly expressed in HCC cells and was positively regulated by the lncRNA HOXD-AS1 in several HCC cell lines. The upregulation of DTNB was significantly associated with T stage, histologic grade, tumour status, adjacent hepatic tissue inflammation, alpha-fetoprotein (AFP) level, and unfavorable prognosis, serving as an independent risk indicator associated with overall survival with substantial diagnostic and prognostic implications for HCC. DTNB was also closely linked to immune cell infiltration, immunotherapy, and sensitivity to anti-HCC drugs. Genes co-expressed with DTNB in HCC were identified, and functional enrichment analysis indicated that DTNB may function in HCC by regulating the cell cycle. A potential ceRNA (competing endogenous RNA) regulatory axis of HOXD-AS1/miR-139-3p/DTNB in HCC was predicted and validated. The high expression of DTNB was validated in our HCC cohort and loss-of-function assays revealed that DTNB knockdown can suppress the proliferation, migration, and invasion of HCC cells and trigger cell cycle arrest at the G0/G1 phase. Conclusions: DTNB, a downstream target of the lncRNA HOXD-AS1, has potential utility as a prognostic biomarker and a target for the treatment of HCC.

Keywords: Hepatocellular carcinoma, DTNB, HOXD-AS1, prognoses, cell cycle

Introduction

Hepatocellular carcinoma (HCC), the foremost histological form of primary liver cancer, is the sixth most common cause of cancer worldwide and the third most common cause of tumour-associated fatalities, posing a significant threat to global public health [1, 2]. Patients in the initial phase of HCC can be effectively treated through surgical resection, liver transplantation, or radiofrequency ablation, but they are susceptible to recurrence and metastasis [3, 4]. Owing to the gradual emergence of HCC and the challenges in its early detection, most HCC patients have progressed to the intermediate and advanced phases before initial diagnosis, missing the opportunity for comprehensive treatment [5]. In the past few years, although molecular targeted drugs (e.g., sorafenib, lenvatinib, etc.) and immune checkpoint inhibitors (e.g., PD-L1 and PD-1 inhibitors) have shown some success in treating advanced HCC, owing to the aggressive phenotype and molecular heterogeneity of HCC, their benefits are limited to a

https://doi.org/10.62347/FCFO5076

select few patients, and the treatment outcomes remain pessimistic [6, 7]. Consequently, it is critically important to develop potent biomarkers for early detection and prognostic assessment of HCC, along with new therapeutic targets for HCC treatment.

Dystrobrevin beta (DTNB), a member of the dystrophin-related protein family, participates in the assembly of the dystrophin-associated protein complex (DPC), which serves as a transmembrane scaffold connecting the cytoskeleton to the extracellular matrix and performs critical functions in preserving the integrity of the muscle fiber surface membrane and modulating intracellular signal transmission [8, 9]. Although DTNB has been identified as a key player in brain development through its regulation of neuronal differentiation, the biological functions of DTNB remain largely unclear [10, 11]. A study revealed that BML-210, an inhibitor of histone deacetylase, is capable of decreasing DTNB expression levels and simultaneously triggering growth suppression and apoptosis in cervical cancer cells [12], implying that DTNB is involved in tumourigenesis and tumour progression.

HOXD cluster antisense RNA 1 (HOXD-AS1), a well-known oncogenic long noncoding RNA (lncRNA), has been demonstrated to facilitate the progression of a range of tumours through modulating cell growth, metastasis, and drug resistance, and represents a robust candidate molecule for the diagnosis and treatment of cancer [13]. A previous study by our research group revealed that the suppression of HOXD-AS1 results in decreased DTNB mRNA levels in HCC cells [14], suggesting that DTNB may contribute to the advancement of HCC as a downstream target of the lncRNA HOXD-AS1. To date, the expression trend of DTNB in HCC and its relevance to HCC are still ambiguous.

This study initially validated the regulatory effect of the lncRNA HOXD-AS1 on DTNB in HCC cells through experiments. A comprehensive analysis was subsequently conducted to systematically elucidate the expression status, clinical relevance, and possible biological roles and mechanisms of DTNB in HCC using bioinformatics techniques and wet-lab examinations. Specifically, this research aimed to lay the foundation for the application of DTNB in the diagnosis and treatment of HCC.

Materials and methods

Human HCC samples

Twenty-five pairs of HCC and adjacent benign liver tissues were collected from patients who underwent surgical resection at the Department of General Surgery of the Second Affiliated Hospital of Xi'an Jiaotong University from 2015 to 2019. Written informed consent was obtained from all patients and this study was approved by the Ethics Committee of the Second Affiliated Hospital of Xi'an Jiaotong University (No. 2022-83).

Cell culture and transfection

The normal human hepatocyte line L-02, along with six HCC cell lines (HepG2, SMMC-7721, MHCC97H, SK-Hep-1, Bel-7402, and Huh7) were acquired from the Cell Bank of the Chinese Academy of Science (Shanghai, China) and propagated at 37°C in an incubator with 5% CO_2 in DMEM supplemented with 10% fetal bovine serum. The lncRNA Smart Silencer, small interfering RNA (siRNA) and microRNA (miRNA) mimics were transfected into cells utilizing the Lipofectamine 3000 reagent (Thermo Fisher Scientific, USA) to knock down the gene expression or overexpress the miRNA. The HOXD-AS1 Smart Silencer (lnc3151204095-343), micrON hsa-miR-139-3p mimic (miR-1180428024312-1-5), and genOFF st-h-DTNB (stB0006192A-1-5) were all acquired from RiboBio (Guangzhou, China).

Quantitative real-time PCR (qRT-PCR)

Total RNA was isolated with RNAzol® RT reagent (Merck, USA) and reverse-transcribed with FastKing gDNA Dispelling RT SuperMix (Tiangen, Beijing, China). qRT-PCR was then carried out with TransStart® Tip Green qPCR SuperMix (+Dye II) (TransGen, Beijing, China), and the relative expression level of the target gene was determined with β-actin as the internal control gene. The following primers were used: HOXD-AS1, 5'-TGTTCCACCAGAAGATTAGAAGTT-3' (forward) and 5'-AGCCCACGCATCTCTATTTG-3' (reverse); DTNB, 5'-CACTCAGTCCGCACCTGTTTT-3' (forward) and 5'-GGTCAGCCATCATTGTGTCTAA-3' (reverse); and β-actin, 5'-TGGCACCCAGCA-CAATGAA-3' (forward) and 5'-CTAAGTCATAGTC-CGCCTAGAAGCA-3' (reverse).

Data acquisition and processing

For pan-cancer analysis, RNA sequencing (RNA-seq) expression data for 18 cancer types were collected from the UCSC XENA (https://xenabrowser.net/datapages/) and the number of samples for each type of cancer is provided in Supplementary Table 1. With respect to HCC, the RNA-seq data, miRNA-seq data and clinical details of 374 HCC samples were acquired from The Cancer Genome Atlas (TCGA) portal (https://portal.gdc.cancer.gov/repository), and the clinical data of each HCC patient are summarized in Supplementary Table 2. The RNA-seq data of 160 normal liver samples were taken from the TCGA database (50 cases) and the Genotype-Tissue Expression project (GTEx; www.gtexportal.org; 110 cases). The Genomics Expression Omnibus (GEO) expression matrices (GSE39791, GSE55092, GSE76427, and GSE54326) were downloaded from the GEO database (https://www.ncbi.nlm.nih.gov/geo/) to confirm the expression status of DTNB in HCC.

Assessment of DTNB/miR-139-3p expression in HCC and their correlations with clinical characteristics

The expression status of DTNB and miR-139-3p across cancers as well as HCC was determined utilizing the R package of "ggplot2". Patients with HCC were categorized into groups with elevated and low expression levels on the basis of the median levels of DTNB or miR-139-3p. A binary logistic regression model was subsequently established to assess the associations between DTNB/miR-139-3p expression and various clinical features, including gender, age, T/N/M stage, histologic grade, tumour status, residual tumour status, the serum alpha-fetoprotein (AFP) level, vascular invasion, the Child-Pugh grade, adjacent hepatic tissue inflammation, and the liver fibrosis Ishak score.

Correlation analysis between DTNB/miR-139-3p and the prognosis in HCC patients

Patients with HCC were categorized into groups with elevated and low expression in terms of the median levels of DTNB or miR-139-3p, and overall survival (OS), disease-specific survival (DSS) and the progression-free interval (PFI) was inspected utilizing the R packages "Survival" and "Survminer". Risk factors influencing OS were then estimated via the Cox proportional hazards regression model, and the clinical features with a *P* value less than 0.1 in the univariate analysis were further integrated into the multivariate test. Additionally, the nomogram prediction model and corresponding calibration curve were created based on risk factors that influence the prognosis via the R packages "rms" and "survival" to predict the of 1-year, 3-year and 5-year OS probabilities.

Assessment of the diagnostic and prognostic performance of DTNB and miR-139-3p in HCC

The diagnostic and prognostic value of DTNB or miR-139-3p was estimated by generating the receiver operating characteristic (ROC) curves and determining the area under the curve (AUC) via the R package "pROC".

Correlation analysis of DTNB with immune infiltration, immune-checkpoint markers, immunotherapy response and chemokines in HCC

The relationship between the DTNB expression and immune infiltration in HCC was investigated utilizing the TCGA data through the single-sample gene set enrichment analysis (ssGSEA) method, which employs the "GSVA" R package [15]. The differential expression of immune checkpoint markers between HCC patients with high and low DTNB expression was determined via the R package "ggplot2". Responses to immunotherapy in HCC patients with high and low DTNB expression were assessed via the tumour immune dysfunction and exclusion (TIDE) algorithm [16]. The correlation between the expression of DTNB and that of 59 chemokine-related genes was examined with the R package "ggplot2".

Correlation analysis of DTNB and anti-tumour drug sensitivity in HCC

The anti-tumour drug sensitivity of each HCC sample was investigated utilizing the data derived from the Genomics of Drug Sensitivity in Cancer (GDSC; https://www.cancerrxgene.org/), a pharmacogenomic database accessible to the public [17]. The link between the expression levels of DTNB and the half-maximal inhibitory concentrations (IC50) of 20 anti-HCC drugs in HCC patients was determined via the R package "pRRophetic". In cases of duplicate gene expression, the expression level was recorded as the average. |Spearman's r| > 0.1 and $P < 0.05$ were considered to indicate a meaningful correlation.

Identification of genes co-expressed with DTNB in HCC

Through batch analysis, genes showing positive co-expression with DTNB in HCC were identified by examining the expression correlation between DTNB and all coding genes (|Spearman's r| > 0.5 and adjusted *p* value < 0.01). Using STRING (www.stringdb.org) and Cytoscape software, the top 10 hub genes were pinpointed by establishing a protein-protein interaction (PPI) network, and their expression and clinical significance in HCC were subsequently examined.

Prediction of DTNB-related biological roles and signaling pathways in HCC

The associations between the top 10 hub genes of DTNB and tumour-related signaling pathways across cancers were analysed with the GSCALite (http://bioinfo.life.hust.edu.cn/web/GSCALite/), a web-based tool for cancer gene set analysis [18]. Genes showing differential expression between HCC patients with high and low DTNB expression were pinpointed via the R package of "DESeq2", and gene set enrichment analysis (GSEA) was carried out based on the MSigDB Collections (https://www.gsea-msigdb.org/) via the "clusterProfiler" R package. The "c5.go.bp.v2022.1.Hs.symbols.gmt" and "c2.cp.all.v2022.1.Hs.symbols.gmt" were adopted as the reference gene sets for Gene Ontology (GO) biological process and Kyoto Encyclopedia of Genes and Genomes (KEGG) pathway analysis, respectively. For each analysis, gene set permutation was performed 1000 times. Statistical significance was determined by a false discovery rate (FDR) of less than 0.05 and an adjusted *P*-value below 0.05.

Western blotting

Total proteins were obtained by lysing the cells with the radioimmunoprecipitation assay (RIPA) buffer (Haigene, Harbin, China) and then separated via sodium dodecyl sulfate-polyacrylamide gel electrophoresis (SDS-PAGE) on 4-20% gradient gels (Beyotime, Shanghai, China). The proteins were subsequently transferred to a polyvinylidene difluoride (PVDF) membrane (0.22 μm) and blocked with Fast Blocking Buffer (Yeasen, Shanghai, China). The membranes were incubated overnight at 4°C with primary antibodies against DTNB (1:1000; PAF385Hu01, Cloud-Clone, USA) and GAPDH (1:1000; 5174T, CST, USA). Following an hour-long exposure to horseradish peroxidase (HRP)-linked goat anti-rabbit IgG (H+L) secondary antibody (1:20,000; 31460, Thermo Fisher Scientific, USA) at ambient temperature, the luminescence signals were detected via an enhanced chemiluminescence (ECL) kit (WBKLS0100, Millipore, USA) and captured via a digital chemiluminescence imager (UVITEC, UK).

Cell Counting Kit-8 (CCK-8) assay

The cells were dispersed into 96-well plates at a density of 4×10^3 cells per well and subjected to a 1 h 30 min incubation at 37°C with CCK-8 reagent (Dojindo, Japan) in accordance with the manufacturer's instructions. The optical density (OD) at a wavelength of 450 nm was measured via a multifunctional microplate reader.

Colony formation assay

The cells were seeded in 6-well plates at a density of 800 cells/well and cultivated in complete medium for one week until they were observed. The colonies were subsequently fixed with 4% paraformaldehyde, stained with 0.1% crystal violet, photographed, and quantified.

Cell cycle assessment by flow cytometry

The cells were fixed in 70% chilled ethanol for an entire night at 4°C, followed by treatment with Hoechst 33342 (10 μg/ml) and RNase A (100 μg/ml). The dyed cells were subsequently analysed via a flow cytometer (CytoFLEX LX, Beckman, USA), and the cell cycle distribution was assessed via FlowJo software (BD Biosciences, USA).

Evaluation of cell migration and invasion by transwell assay

The capacities of cell migration and invasion, respectively, were examined with transwell chambers with and without a Matrigel coating in 24-well plates (8.0 μm, polyester membrane, 353097/354480, Corning, USA). The density of the cells was adjusted to 2.5×10^5 cells/ml using serum-free medium, 200 μl of the cell suspension was added to the top chamber, and culture medium supplemented with 10% FBS was added to the bottom chamber as a chemo-

tactic factor. Following a 24 h (migration) or 48 h (invasion) culture period, the cells on the inner surface of the PET membrane were removed, and the membranes were fixed with 4% paraformaldehyde and stained with crystal violet. The cells that passed through the membrane were subsequently imaged under a microscope.

Statistical analysis

Statistical evaluation was performed via R software (v.4.2.1) and SPSS 26.0. The differences in the expression of DTNB and miR-139-3p in unpaired and paired samples were examined via the Mann-Whitney U test and the Wilcoxon signed-rank test, respectively. The association between DTNB/miR-139-3p expression and clinical parameters was investigated by logistic regression analysis. To ascertain whether there was any difference in survival probability between the high and low DTNB/miR-139-3p expression groups, a Kaplan-Meier analysis was conducted via the log-rank test. The clinicopathological characteristics linked to OS were pinpointed by performing univariate and multivariate Cox regression analyses. The association between the expression of the two genes was assessed via Spearman's correlation test. A *P*-value less than 0.05 was considered to indicate a significant difference.

Results

DTNB was elevated by the oncogenic lncRNA HOXD-AS1 in HCC cells

Our previous RNA-seq investigation revealed that silencing the oncogenic lncRNA HOXD-AS1 resulted in a reduction in DTNB expression in the Bel-7402 HCC cell line (**Figure 1A**). To validate the regulatory influence of HOXD-AS1 on DTNB in HCC cells, the expression of HOXD-AS1 and DTNB in six human HCC cell lines (HepG2, Bel-7402, SMMC-7721, MHCC97H, SK-Hep-1, and Huh7) as well as the normal hepatocyte line L-02 were assessed via qRT-PCR, and the results revealed that the expression levels of HOXD-AS1 and DTNB were notably elevated in all six HCC cell lines compared with those in the human normal liver cell line L-02 (**Figure 1B**), indicating that HOXD-AS1 and DTNB had similar expression trends in HCC cells. Next, the impact of HOXD-AS1 on DTNB expression in HCC cell lines was explored. HOXD-AS1 was effectively knocked down in all six HCC cell lines (**Figure 1C**) and the DTNB expression level was significantly reduced by HOXD-AS1 suppression (**Figure 1D**), suggesting that HOXD-AS1 positively regulates DTNB expression in HCC. In addition, the TCGA data also revealed a positive relationship between HOXD-AS1 and DTNB expression in HCC samples, which aligns with the above experimental findings (**Figure 1E**).

DTNB was highly expressed in HCC tissues

To investigate the expression trends of DTNB in HCC patients, first, RNA-seq data derived from the TCGA and GTEx databases, including data from 374 HCC tissues samples, 160 normal tissues samples, and 50 paired normal-HCC tissues samples, were used to estimate the expression of DTNB, and the findings revealed that DTNB was dramatically elevated in cancerous tissues, relative to normal tissues ($P < 0.001$) (**Figure 2A**, **2B**). The expression of DTNB in HCC tissues was subsequently examined via GEO data, and we found that in all four GEO datasets used for validation, the expression levels of DTNB were notably greater in tumour samples than in normal tissues ($P < 0.001$) (**Figure 2C-F**). Thus, the above findings suggest that DTNB is upregulated in HCC tissues.

Furthermore, the expression status of DTNB was further investigated in pan-cancer patients employing RNA-seq data from TCGA corresponding to 18 cancer types. As illustrated in **Figure 2G**, DTNB was abnormally expressed in most cancer types except for BRCA and PAAD. DTNB was overexpressed in 13 cancer types (BLCA, CHOL, COAD, ESCA, HNSC, KIRP, HCC, LUAD, LUSC, PRAD, READ, STAD, and UCEC), whereas it was downregulated in only three cancer types, namely, KICH, KIRC, and THCA. In addition, paired comparison analysis confirmed increased expression of DTNB in BLCA, CHOL, COAD, ESCA, HCC, LUSC, PRAD, STAD, and UCEC in contrast to its reduced expression in KICH, KIRC, and THCA (**Figure 2H**).

Associations between DTNB expression and the clinical features of HCC patients

The associations between DTNB expression and clinicopathological variables in HCC patients were assessed by constructing a binary logistic regression model. As shown in **Figure 3**, high DTNB levels in HCC tissues were strongly positively correlated with T stage (OR=1.803,

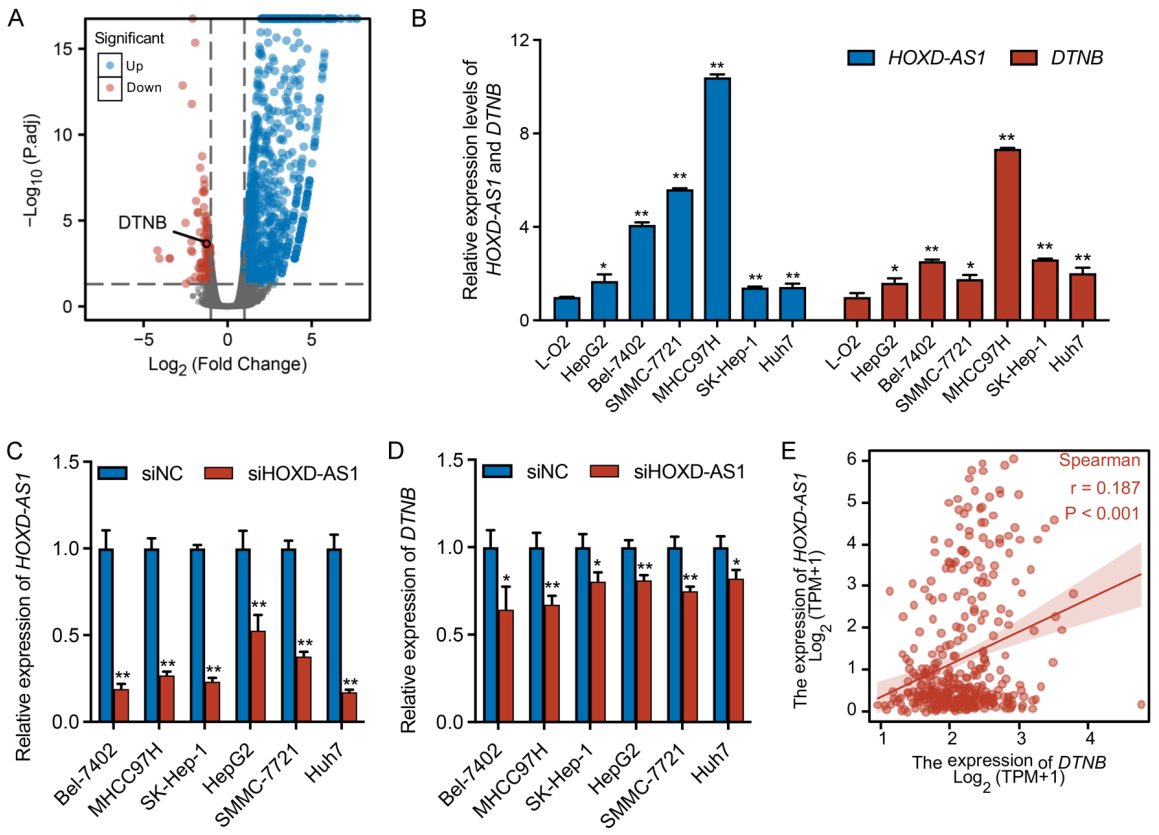

Figure 1. DTNB was upregulated by the oncogenic lncRNA HOXD-AS1 in HCC cells. A. Our previous RNA-seq results showed that the expression level of DTNB could be reduced by HOXD-AS1 silencing [14]. B. The expression of HOXD-AS1 and DTNB in HCC cell lines was determined by qRT-PCR. C. Knockdown efficiency of HOXD-AS1 in HCC cell lines was evaluated via qRT-PCR. D. The effect of HOXD-AS1 knockdown on DTNB expression in HCC cell lines was assessed via qRT-PCR. E. The correlation between the expression of HOXD-AS1 and DTNB was analysed based on the TCGA data. *P < 0.05, **P < 0.01.

P=0.016), histological grade (OR=1.884, P=0.004), tumour status (OR=1.640, P=0.022), adjacent hepatic tissue inflammation (OR=1.829, P=0.022), and AFP levels (OR=3.558, P < 0.001). Collectively, the above findings imply that high DTNB expression levels are closely related to poor clinicopathological characteristics.

Association between the expression of DTNB and the prognosis of HCC patients

To determine the correlation between DTNB expression and the prognosis of HCC patients, we categorized the HCC patients into high- and low-expression groups in accordance with the median DTNB expression, and the variations in OS, DSS, and PFI between the two groups were analysed. As illustrated in **Figure 4A-C**, HCC patients with high DTNB expression levels had markedly lower OS, DSS, and PFI than did those with low DTNB expression levels (both P < 0.05), indicating that elevated DTNB expression is an unfavorable predictor in HCC. Univariate Cox regression analysis revealed that the DTNB expression level (HR=1.977, P < 0.001), T stage (HR=2.540, P < 0.001), M stage (HR=4.032, P=0.018), and tumour-bearing status (HR=2.361, P < 0.001) were strongly correlated with the OS of HCC patients (**Figure 4D**). Multivariate Cox regression assessment further disclosed that the expression level of DTNB (HR=1.707, P=0.021) was independently correlated with OS in patients with HCC (**Figure 4E**). Furthermore, a nomogram prediction model was established by incorporating the prognostic risk factors of the DTNB expression level, T stage, M stage, and tumour status to forecast the 1-, 3-, and 5-year OS probabilities of HCC patients (**Figure 4F**), which was highly accurate and stable during the calibration tests (**Figure 4G**).

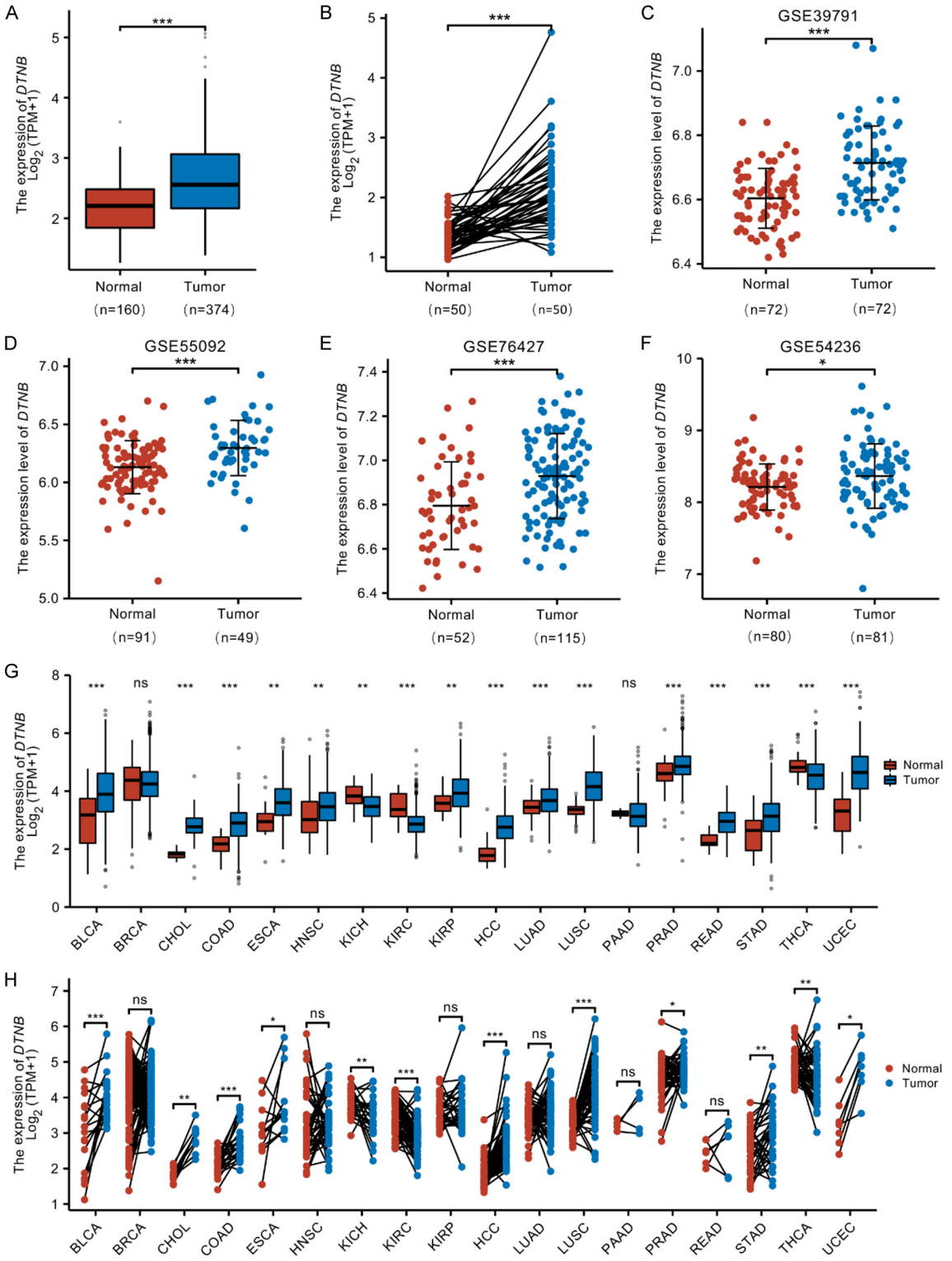

Figure 2. DTNB was upregulated in HCC tissues. The expression status of DTNB in unpaired (A) and paired (B) HCC tissues were analyzed using the TCGA data and validated in four GEO datasets (C-F). Pan-cancer analysis of DTNB expression in unpaired (G) and paired (H) tissues across 18 cancer types. *$P < 0.05$, **$P < 0.01$, ***$P < 0.001$. NS, no significance; BRCA, breast invasive carcinoma; BLCA, bladder urothelial carcinoma; CHOL, cholangiocarcinoma; COAD, colon adenocarcinoma; ESCA, esophageal carcinoma; HNSC, head and neck squamous cell carcinoma; KICH, kidney chromophobe; KIRC, kidney renal clear cell carcinoma; KIRP, kidney renal papillary cell carcinoma; LUAD, lung adenocarcinoma; LUSC, lung squamous cell carcinoma; PAAD, pancreatic adenocarcinoma; PRAD, prostate adenocarcinoma; READ, rectum adenocarcinoma; STAD, stomach adenocarcinoma; THCA, thyroid carcinoma; UCEC, uterine corpus endometrial carcinoma.

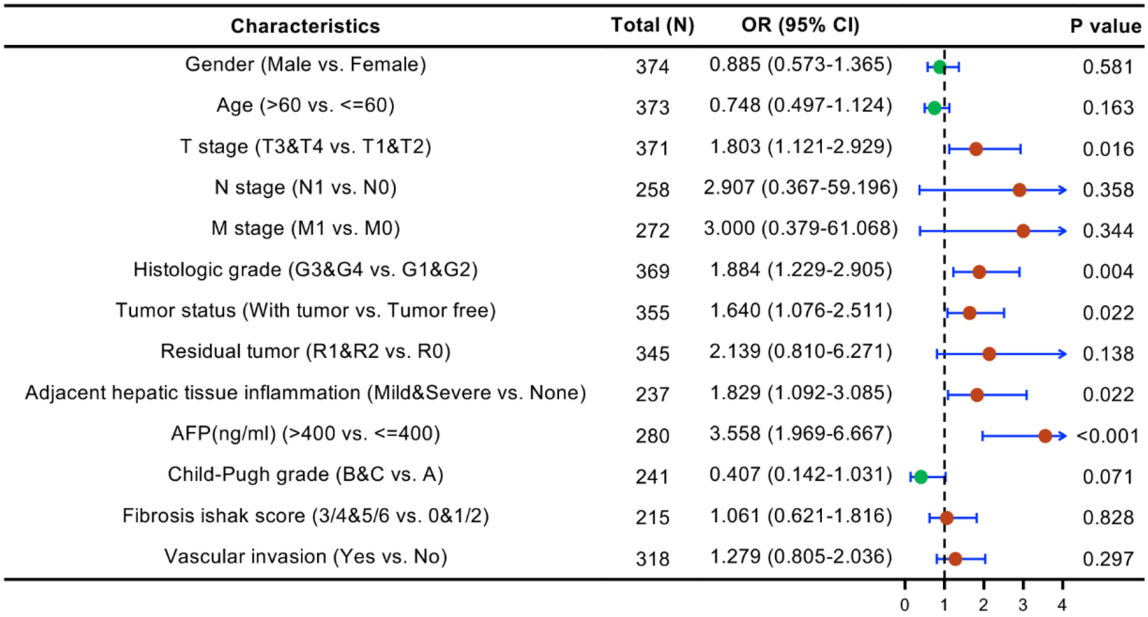

Figure 3. The association between DTNB expression and clinicopathologic characteristics of the HCC patients was evaluated by logistic regression analysis. AFP, alpha-fetoprotein; CI, confidence interval; OR, odd ratio.

Diagnostic and prognostic value of DTNB in HCC

ROC curves were plotted to assess the diagnostic value of the DTNB expression in HCC. As illustrated in **Figure 5A-D**, the DTNB expression level was favorable for the diagnosis of HCC (AUC=0.931), T1-T2 stage (AUC=0.929), histological stage G1-G2 (AUC=0.924), and tumour status (AUC=0.932). Furthermore, the DTNB expression level was also effective in predicting the 1-, 3-, and 5-year OS (AUC=0.691, 0.638, and 0.604), DSS (AUC=0.729, 0.642, and 0.556), and PFI (AUC=0.648, 0.582, and 0.611) (**Figure 5E-G**).

Relevance of DTNB expression to immune infiltration, immune checkpoint markers, immunotherapy response and chemokine-related genes in HCC

The relationship between the DTNB expression and the degree of infiltration of 19 immune cell types in HCC tissues was examined (**Figure 6A**), and a strong relationship was revealed between DTNB expression and the infiltration of four types of immune cells in the HCC tumour microenvironment (|Spearman's r| > 0.2, $P < 0.05$). Specifically, there was a positive correlation with the infiltration of Th2 cells (**Figure 6B**), whereas negative associations were observed with the infiltration of plasmacytoid dendritic cells (pDC), neutrophils, and Th17 cells (**Figure 6C-E**). Notably, several immune checkpoint markers, including PD-L1, CTLA4, HAVCR2, LAG3, PD-1, PDCD1LG2, and TIGIT, were dramatically increased in HCC patients with upregulated DTNB (**Figure 6F**). The predictive value of the DTNB expression level for immunotherapy outcomes in HCC patients was assessed using the TIDE score calculation, revealing that the group with elevated DTNB expression presented a notably higher TIDE score (**Figure 6G**). Furthermore, a positive association was observed between the expression of DTNB and the expression of most chemokine-related genes in HCC tissues (|Spearman's r| > 0.1, $P < 0.05$) (**Figure 7A** and Supplementary Table 3), including CCR3, CCR10, XCL1, CCL28, CXCR4, CXCL11, CXCR3, CCL26, CXCL3, CCR1, and CCL20 (**Figure 7B**).

Correlation between DTNB expression and responsiveness to antitumour drugs in HCC

Using the GDSC database, we assessed the correlation between DTNB expression in HCC patients and sensitivity to 20 chemotherapy and targeted drugs used in HCC therapy. As illustrated in **Figure 8**, except for gefitinib, lapatinib, and mitomycin C, the IC50 values of the remaining 17 drugs exhibited a notable link with the expression of DTNB in HCC. Specifically, there was an inverse relationship between the

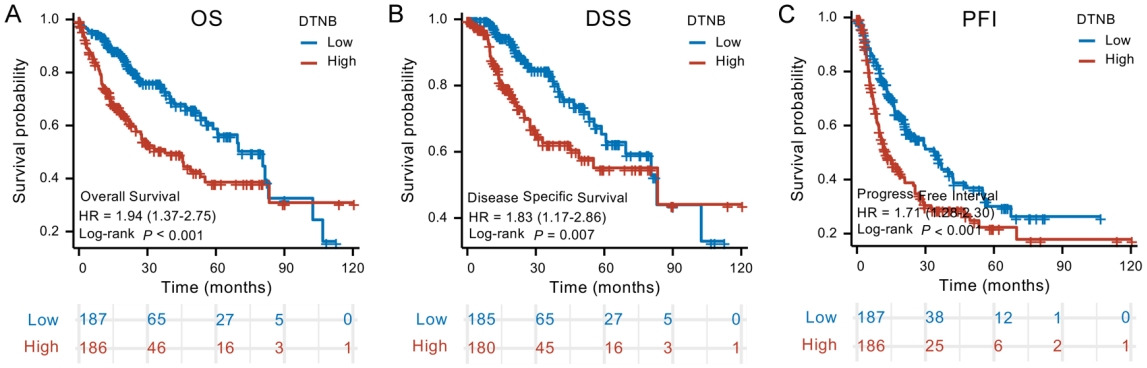

D

Characteristics	Total (N)	HR (95% CI)	P value
T stage (T3&T4 vs. T1&T2)	367	2.540 (1.785 - 3.613)	<0.001
M stage (M1 vs. M0)	270	4.032 (1.267 - 12.831)	0.018
Tumor status (With tumor vs. Tumor free)	351	2.361 (1.620 - 3.441)	<0.001
DTNB (Low vs. High)	370	1.977 (1.390 - 2.811)	<0.001
N stage (N1 vs. N0)	256	2.004 (0.491 - 8.181)	0.333
Gender (Male vs. Female)	370	0.816 (0.573 - 1.163)	0.26
Age (>60 vs. <=60)	370	1.248 (0.880 - 1.768)	0.214
Residual tumor (R1&R2 vs. R0)	341	1.571 (0.795 - 3.104)	0.194
Histologic grade (G3&G4 vs. G1&G2)	365	1.120 (0.781 - 1.606)	0.539
Adjacent hepatic tissue inflammation (Mild&Severe vs. None)	233	1.228 (0.755 - 1.997)	0.409
AFP(ng/ml) (>400 vs. <=400)	277	1.056 (0.646 - 1.727)	0.827
Child-Pugh grade (B&C vs. A)	238	1.616 (0.797 - 3.275)	0.183
Fibrosis ishak score (3/4&5/6 vs. 0&1/2)	211	0.757 (0.455 - 1.260)	0.285
Vascular invasion (Yes vs. No)	314	1.348 (0.890 - 2.042)	0.159

E

Characteristics	Total (N)	HR (95% CI)	P value
T stage (T3&T4 vs. T1&T2)	367	2.328 (1.478 - 3.666)	< 0.001
M stage (M1 vs. M0)	270	1.027 (0.242 - 4.353)	0.971
Tumor status (With tumor vs. Tumor free)	351	1.985 (1.243 - 3.171)	0.004
DTNB (Low vs. High)	370	1.707 (1.084 - 2.689)	0.021

F

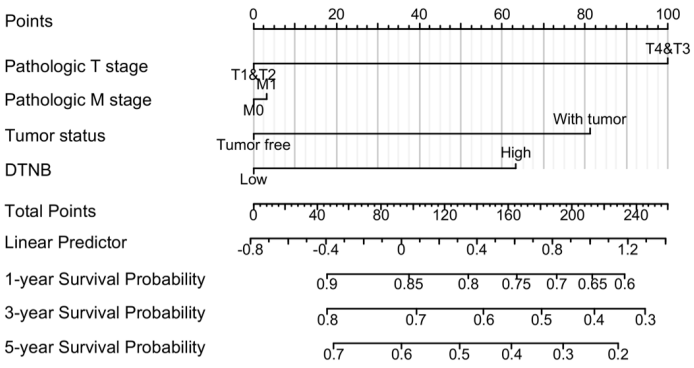

G

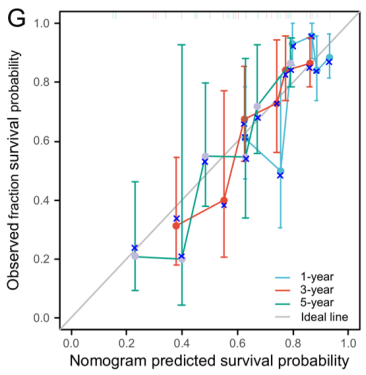

Figure 4. The association of DTNB expression with the prognosis of HCC patient. Kaplan-Meier survival curves display the relationship of DTNB expression with overall survival (A), disease specific survival (B) and progression-free interval (C). Forest plot showing results of univariate (D) and multivariate (E) Cox regression analysis of DTNB expression level for overall survival. (F) The nomogram predicting 1-, 3- and 5-year overall survival. (G) Calibration curves of the nomogram prediction model. AFP, alpha-fetoprotein; CI, confidence interval; DSS, disease-specific survival; HR, hazard ratio; OS, overall survival; PFI, progression-free interval.

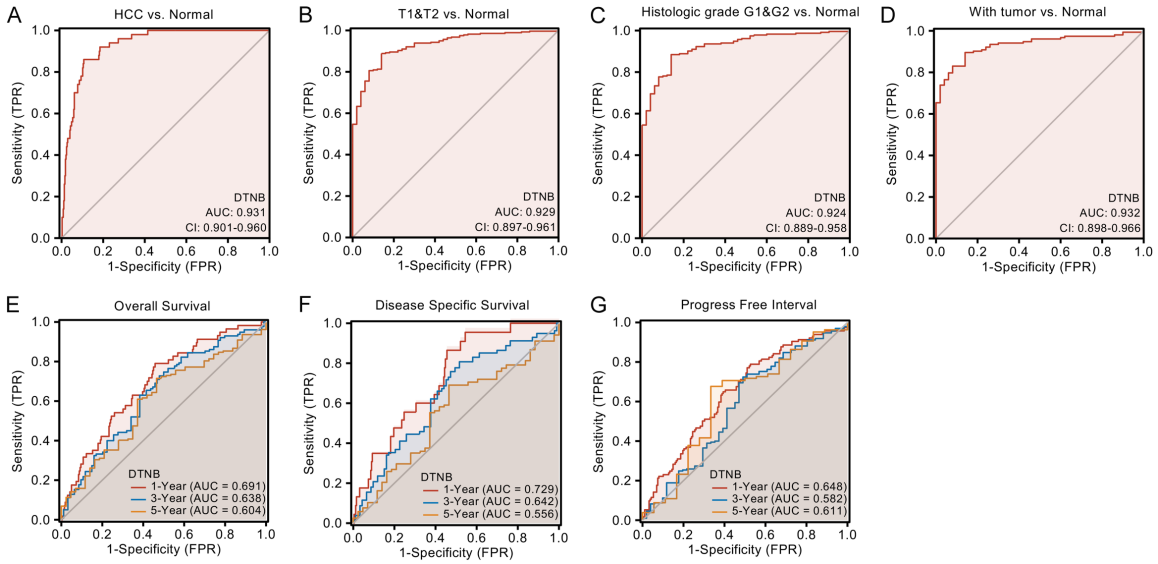

Figure 5. Diagnostic and prognostic ROC curves of DTNB in HCC. A. HCC vs. normal. B. T1&T2 stage vs. normal. C. Histologic grade G1&G2 vs. normal. D. With tumour vs. normal. E. 1-, 3-, and 5-year overall survival. F. 1-, 3-, and 5-year disease specific survival. G. 1-, 3-, and 5-year progression-free interval. AUC, area under the curve; CI, confidence interval; FRP, false positive rate; TRP, true positive rate.

DTNB expression levels and the IC50 values of 5-fluorouracil (r=-0.42, $P < 0.001$), axitinib (r=-0.48, $P < 0.001$), camptothecin (r=-0.34, $P < 0.001$), cisplatin (r=-0.11, $P=0.036$), doxorubicin (r=-0.23, $P < 0.001$), foretinib (r=-0.22, $P < 0.001$), gemcitabine (r=-0.38, P < 0.001), imatinib (r=-0.31, P < 0.001), methotrexate (r=-0.44, $P < 0.001$), paclitaxel (r=-0.41, $P < 0.001$), pazopanib (r=-0.23, $P < 0.001$), rapamycin (r=-0.12, $P=0.02$), sorafenib (r=-0.30, $P < 0.001$), tivozanib (r=-0.34, $P < 0.001$) and vinorelbine (r=-0.60, $P < 0.001$), but a positive association was noted with cetuximab (r=0.40, $P < 0.001$) and erlotinib (r=0.38, $P < 0.001$). Collectively, the above findings imply that the DTNB expression in patients with HCC is closely linked to the sensitivity to the aforementioned antitumour drugs.

Prediction of DTNB-related biological functions and signaling pathways in HCC

To gain insight into the underlying biological roles and signaling pathways of DTNB in HCC, first, the positively co-expressed genes (PCEGs) of DTNB were identified, and 1153 genes were ultimately confirmed to be strongly positively co-expressed with DTNB in HCC (|Spearman's r| > 0.5, adjusted P value < 0.01; Supplementary Table 4). Next, the 10 hub genes (BUB1, CDK1, DLGAP5, KIF2C, CCNB1, BUB1B, CDC20, KIF11, KIF20A, and ASPM) were clarified through constructing a network of protein-protein interactions employing the PCEGs of DTNB (**Figure 9A**), and their expression exhibited a robust positive relationship with DTNB in HCC (**Figure 9B**, **9C**). Clinical correlation analysis uncovered that these 10 hub genes were significantly elevated in HCC (**Figure 10A**) and were positively correlated with pathologic T stage and histological grade (both $P < 0.01$) (**Figure 10B**, **10C**). These 10 hub genes were further revealed to be negatively associated with the OS of patients with HCC (both $P < 0.05$) (**Figure 11A**) and exhibited favorable predictive significance for 1-, 3-, and 5-year OS (all AUC > 0.5) (**Figure 11B**). The associations between the 10 hub genes of DTNB and several tumour-

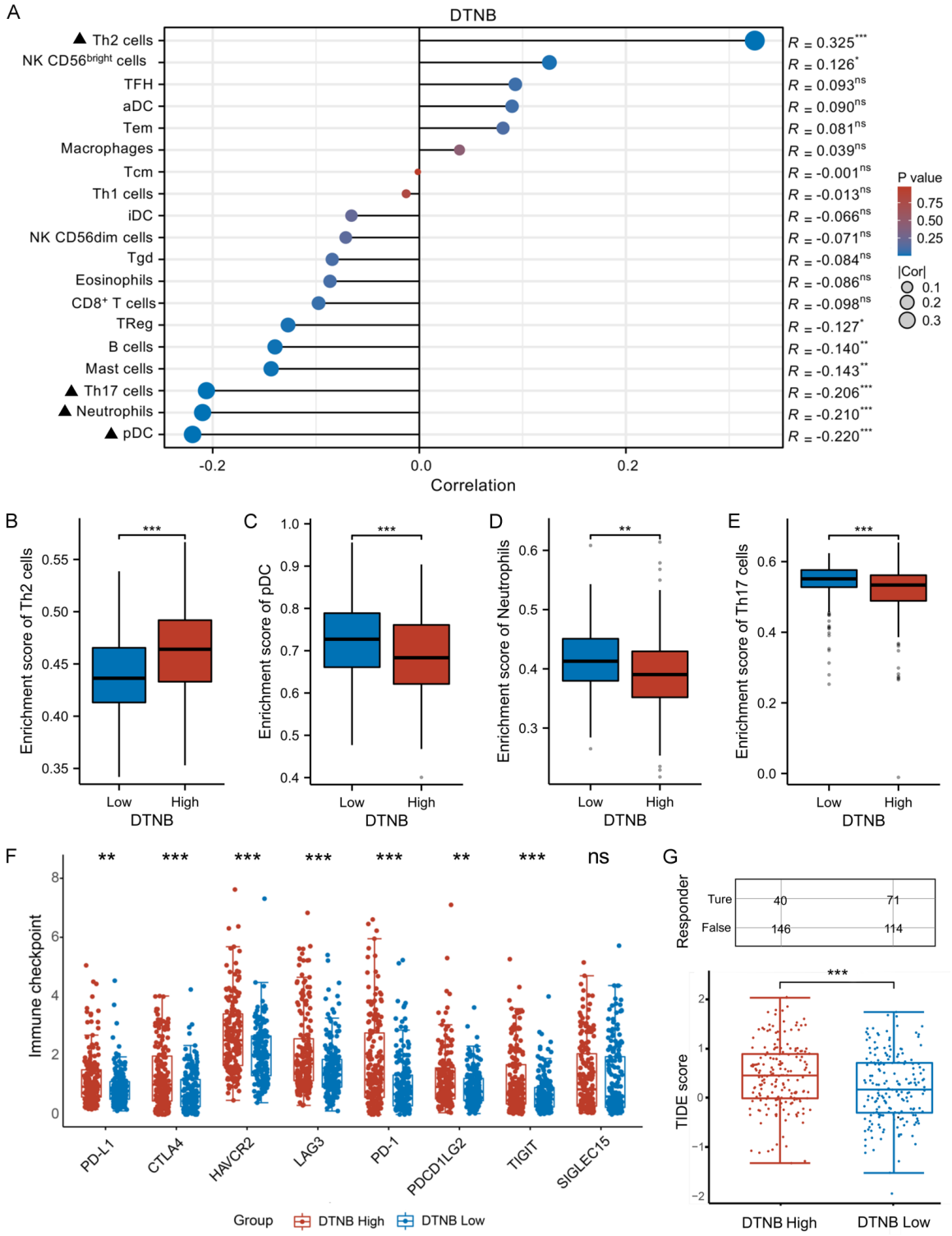

Figure 6. The relationship of DTNB expression with the immune cell infiltration and immunotherapy response in HCC. (A) The lollipop chart shows the correlation between the DTNB expression level and the infiltration of 19 types of immune cells. The black triangle (▲) represents infiltrating immune cell types significantly associated with DTNB expression (|Spearman's r| > 0.2, $P < 0.05$). The infiltration levels of Th2 cells (B), pDC (C), neutrophils (D) and Th17 cells (E) in different DTNB expression groups. The association of DTNB expression with immune checkpoint markers (F) and tumour immune dysfunction and exclusion (TIDE) scores (G) in HCC was evaluated. *$P < 0.05$, **$P < 0.01$, ***$P < 0.001$. NS, no significance.

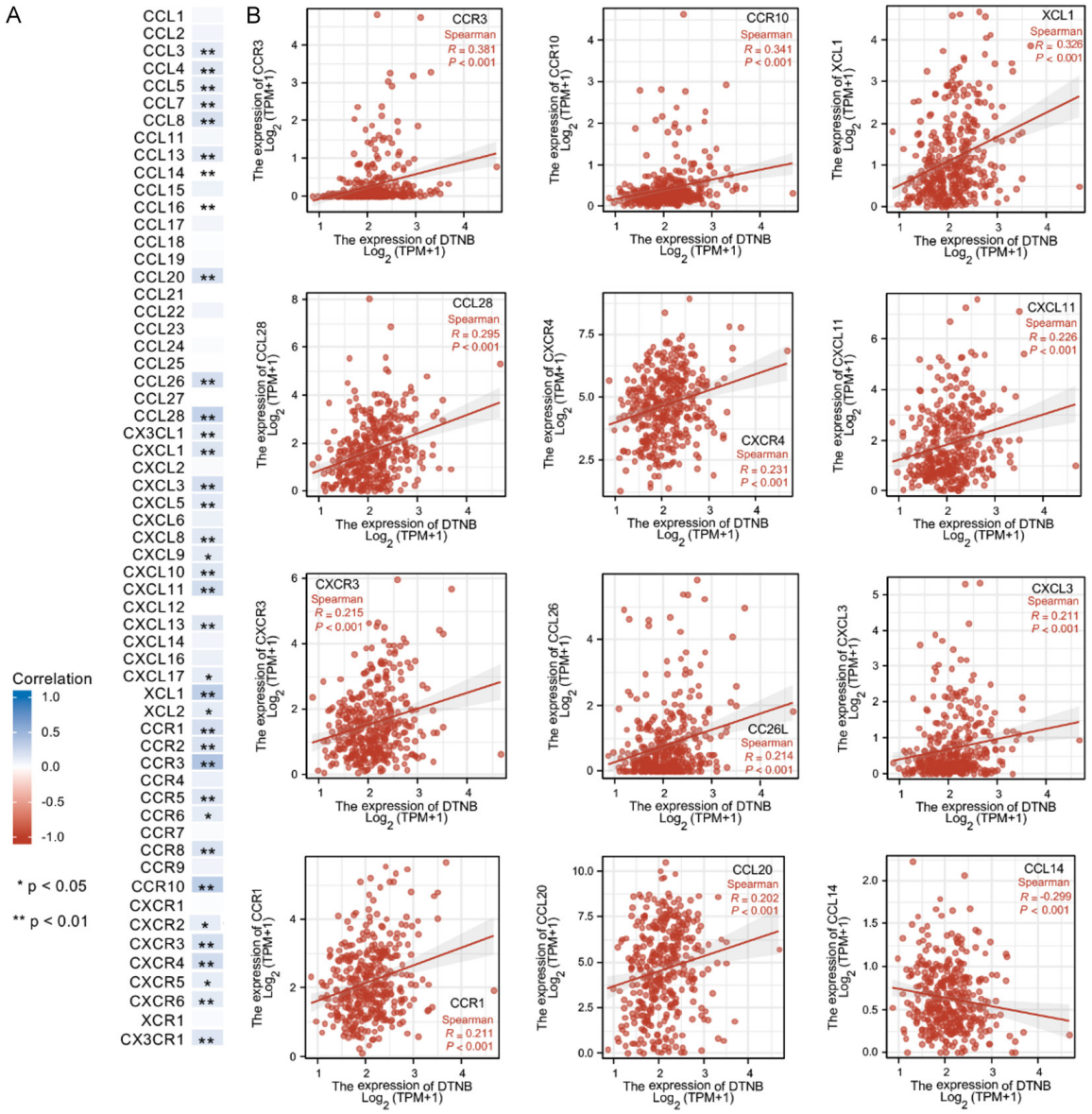

Figure 7. The correlation between DTNB expression and chemokine-related genes. A. The heatmap shows the correlation between the expression of DTNB and 59 chemokine-related genes in HCC, and the asterisk (* or **) represent genes whose expression are significantly associated with DTNB (|Spearman's r| > 0.1, $P < 0.05$). B. The scatterplot shows the relationship of the expression of DTNB and 12 representative chemokine-related genes (|Spearman's r| > 0.2, $P < 0.05$). *$P < 0.05$, **$P < 0.01$.

related signalling pathways in pan-cancer were subsequently explored via GSCALite, and the results indicated that DTNB and the genes most closely related to DTNB were closely related to the regulation of the cell cycle and apoptosis (**Figure 12A**).

Moreover, GSEA-based GO and KEGG enrichment between low and high DTNB expression datasets in HCC was also carried out, and the criteria of FDR < 0.05 and adjusted *P* value < 0.05 were used to indicate marked differences in enrichment (Supplementary Tables 5 and 6). As shown in **Figure 12B** and **12C**, the top 10 enriched GO biological process terms in the group with high DTNB expression were predominantly associated with B cell activation and cell cycle-related processes, and the top 10 enriched KEGG pathways in the group with high DTNB expression were also related to immune regulation and the cell cycle. Taken together, the above results indicate that DTNB may con-

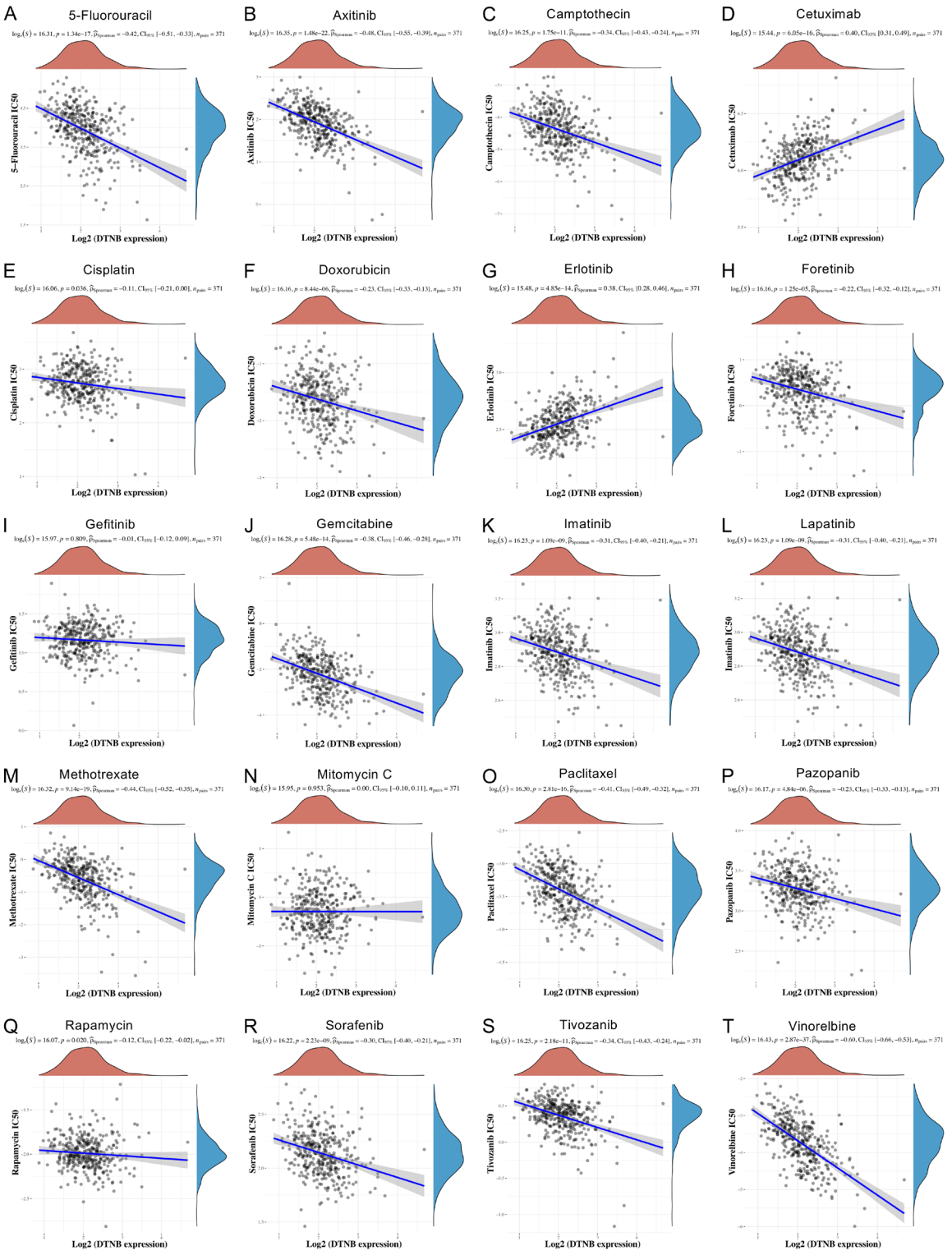

Figure 8. The correlation of DTNB expression with IC50 values of 20 anti-HCC drugs based on the GDSC data. A. 5-Fluorouracil. B. Axitinib. C. Camptothecin. D. Cetuximab. E. Cisplatin. F. Doxorubicin. G. Erlotinib. H. Foretinib. I. Gefitinib. J. Gemcitabine. K. Imatinib. L. Lapatinib. M. Methotrexate. N. Mitomycin C. O. Paclitaxel. P. Pazopanib. Q. Rapamycin. R. Sorafenib. S. Tivozanib. T. Vinorelbine.

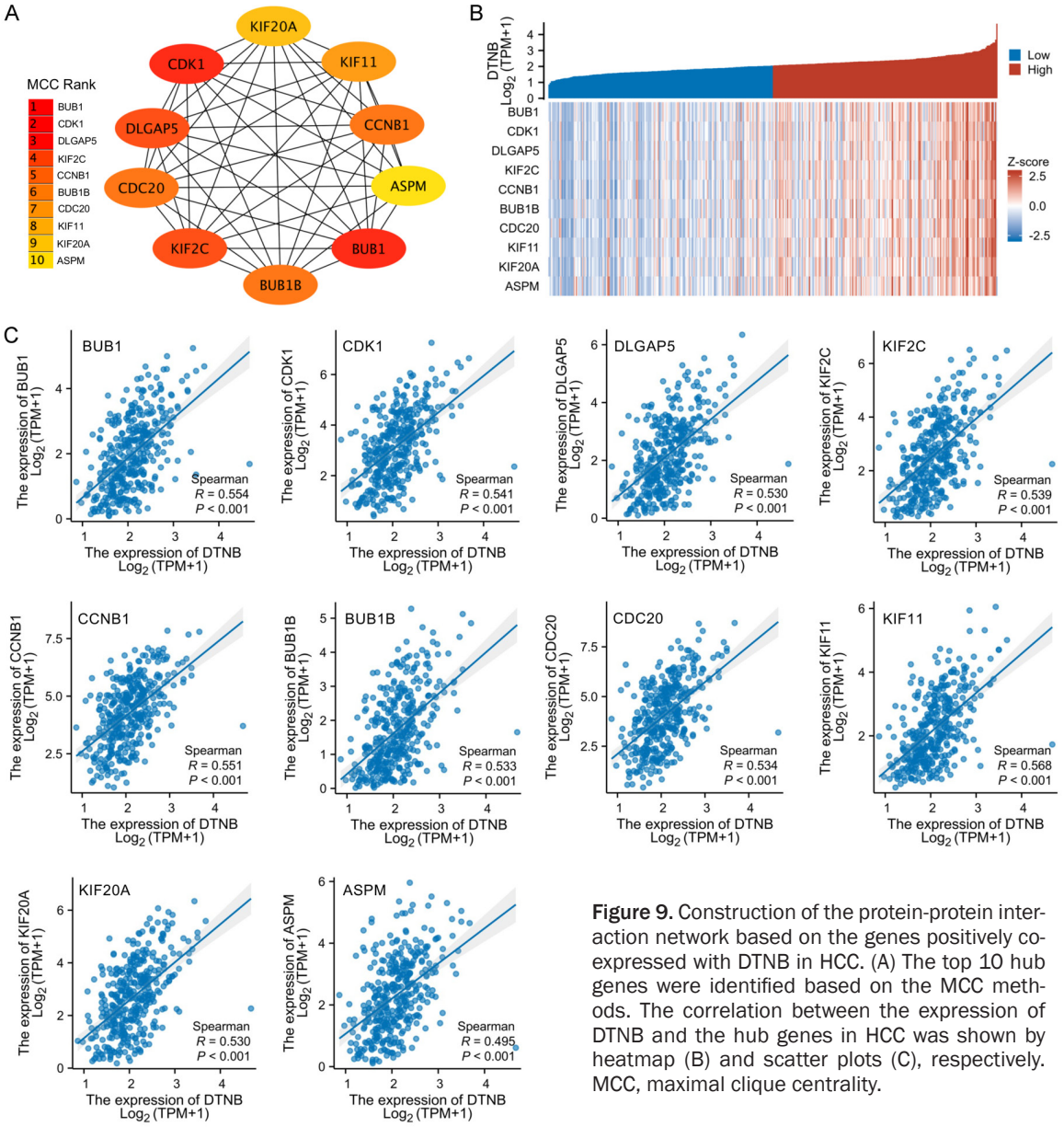

Figure 9. Construction of the protein-protein interaction network based on the genes positively co-expressed with DTNB in HCC. (A) The top 10 hub genes were identified based on the MCC methods. The correlation between the expression of DTNB and the hub genes in HCC was shown by heatmap (B) and scatter plots (C), respectively. MCC, maximal clique centrality.

tribute to the HCC progression by modulating the cell cycle.

Identification of a potential competing endogenous RNA (ceRNA) regulatory axis of HOXD-AS1/miR-139-3p/DTNB in HCC

HOXD-AS1 has been demonstrated to mo dulate its downstream genes via a ceRNA mechanism [19, 20]. Here, we explored the potential miRNAs that can constitute the ceRNA regulatory axis together with HOXD-AS1 and DTNB. The potential miRNAs targeting HOXD-AS1 and DTNB were obtained via the DIANA LncBase v2.0, and miRWalk databases, respectively (Supplementary Tables 7 and 8), and then intersected with miRNAs that were negatively related to the OS of HCC patients (Supplementary Table 9). Finally, miR-139-3p was screened for its potential to form a ceRNA regulatory axis with HOXD-AS1 and DTNB (**Figure 13A**, **13B**). Bioinformatics analysis disclosed that miR-139-3p was modestly expressed in HCC tissues and that its expression exhibited an inverse relationship with both HOXD-AS1 and DTNB (**Figure 13C**, **13D**). Clinical significance analysis revealed that decreased expression of miR-139-3p was positively related to the histological grade, APF

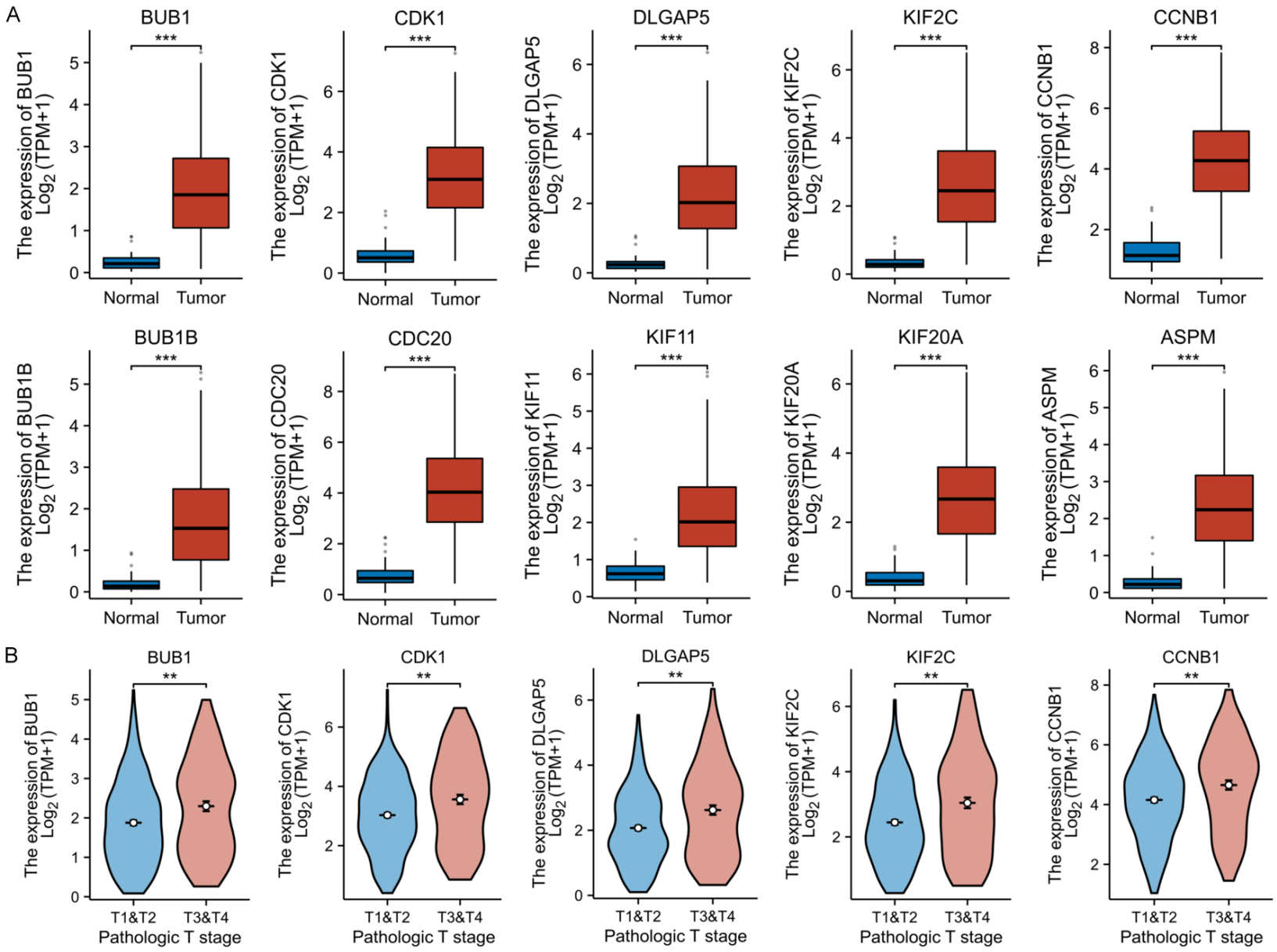
A
BUB1
CDK1
DLGAP5
KIF2C
CCNB1
BUB1B
CDC20
KIF11
KIF20A
ASPM
***
The expression of BUB1 Log2 (TPM+1)
The expression of CDK1 Log2 (TPM+1)
The expression of DLGAP5 Log2 (TPM+1)
The expression of KIF2C Log2 (TPM+1)
The expression of CCNB1 Log2 (TPM+1)
The expression of BUB1B Log2 (TPM+1)
The expression of CDC20 Log2 (TPM+1)
The expression of KIF11 Log2 (TPM+1)
The expression of KIF20A Log2 (TPM+1)
The expression of ASPM Log2 (TPM+1)
Normal
Tumor
B
**
T1&T2
T3&T4
Pathologic T stage

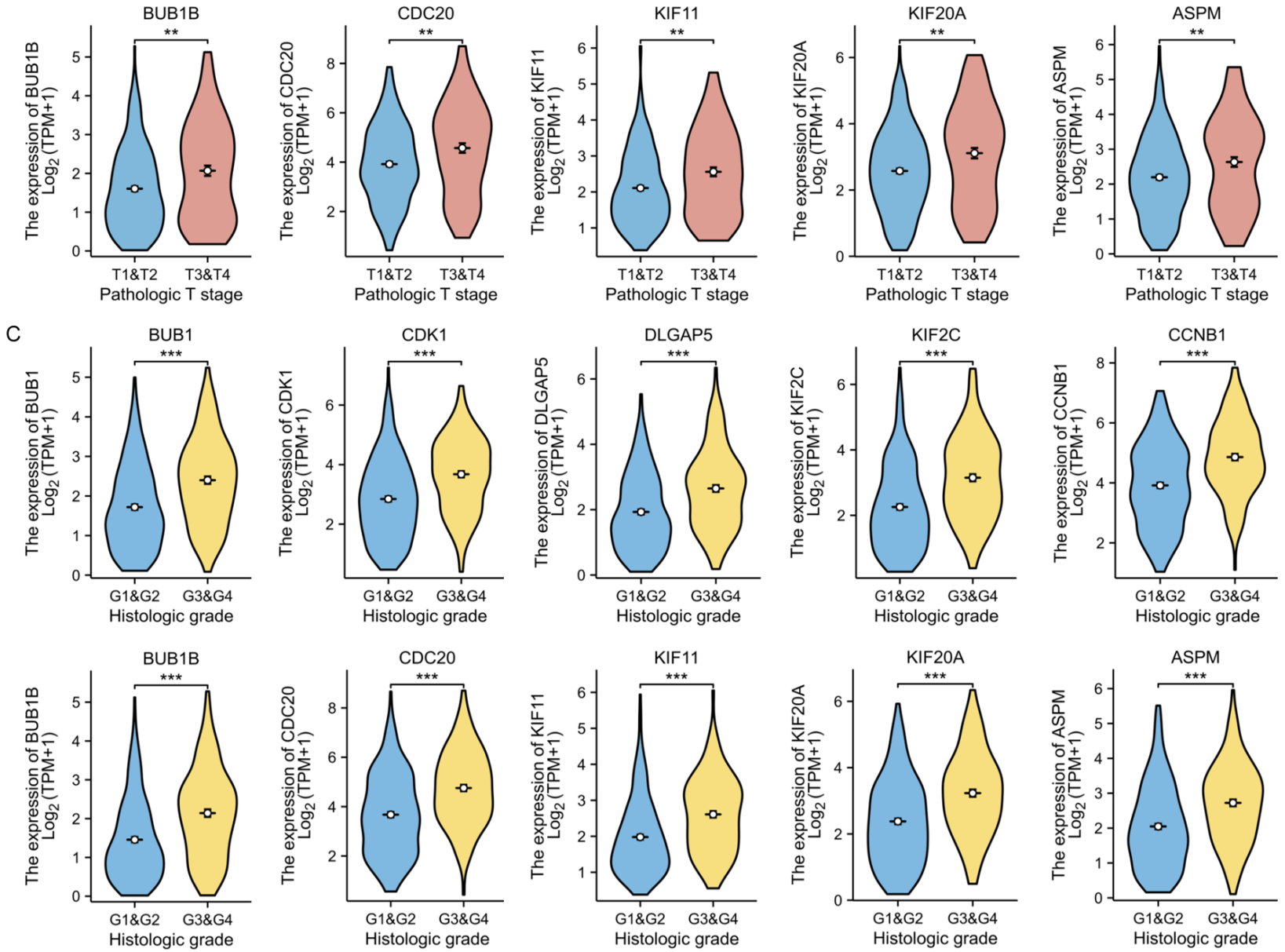

Figure 10. The expression status of the top 10 hub genes in HCC (A) and their correlation with pathologic T stage (B) and histological grade (C). $^{**}P < 0.01$, $^{***}P < 0.001$.

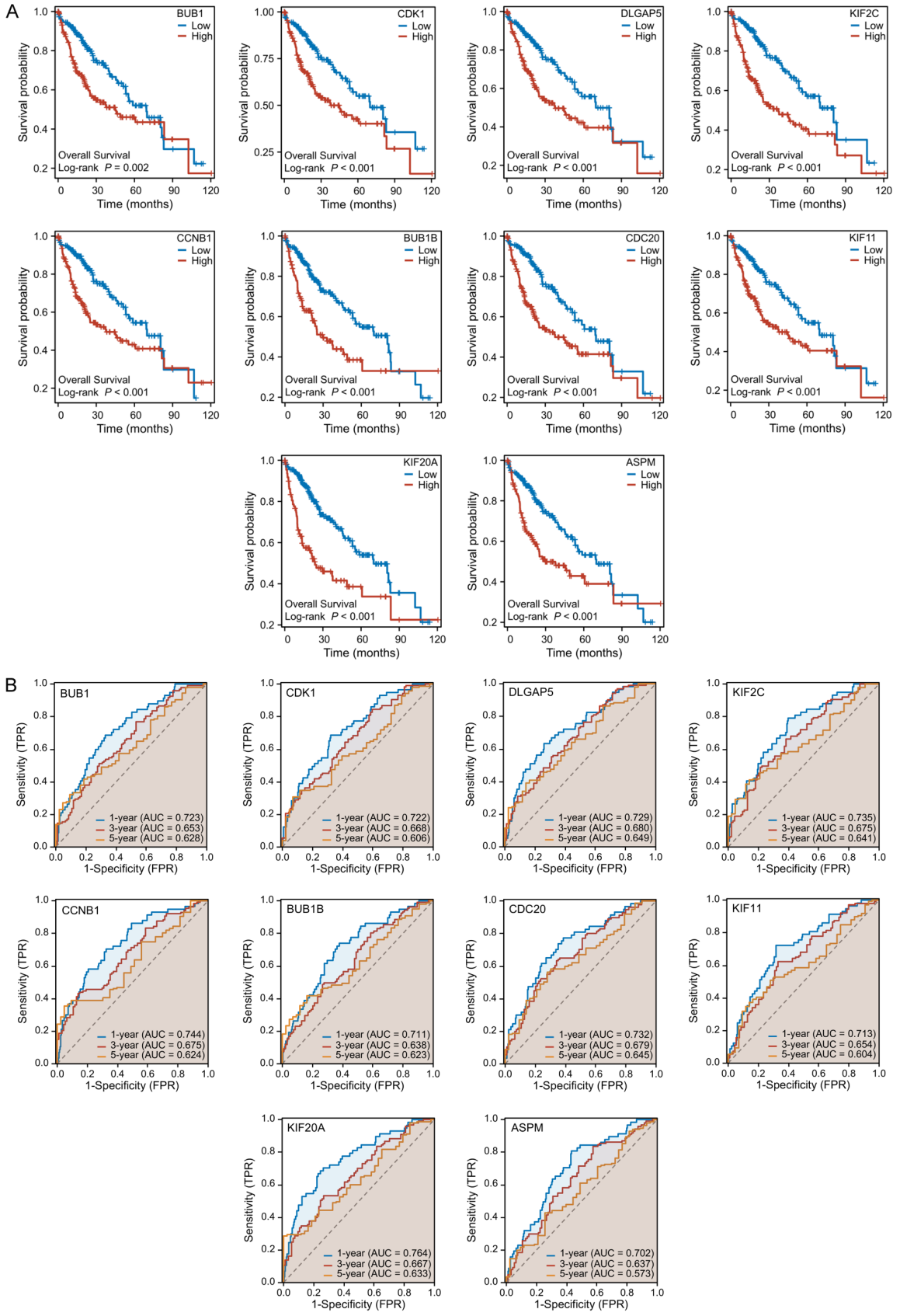

Figure 11. The correlation of the hub genes expression with overall survival (A) and their predictive efficacy for 1-, 3-, 5-year overall survival (B) in HCC. AUC, area under the curve; TPR, true-positive rate; FPR, false-positive rate.

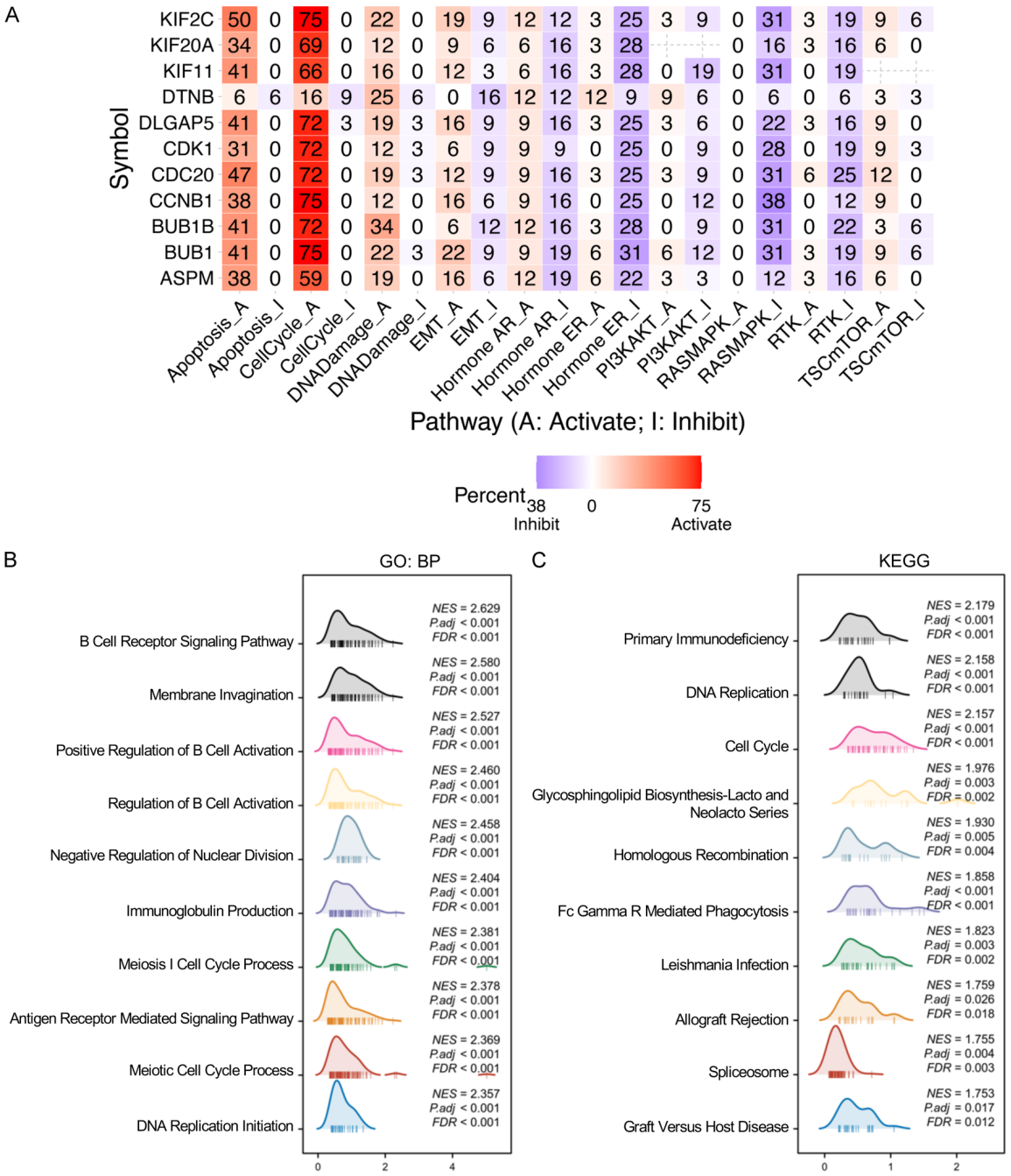

Figure 12. Prediction of DTNB-related biological functions and signaling pathways in HCC. A. The association of DTNB and the top 10 hub genes with some tumour-related signaling pathways in pan-cancer was analysed by GSCALite. B. The top 10 significantly enriched GO biological process terms in the high DTNB expression group. C. The top 10 significantly enriched KEGG pathways in the high DTNB expression group. BP, biological process; FDR, false discovery rate; NES, normalized enrichment scores; *P*. adj, adjusted *P*-values.

level, and unfavorable prognosis of HCC patients and was an independent risk indicator influencing the OS of HCC patients (**Figure 13E-G**). The ROC curve uncovered that miR-139-3p expression had excellent diagnostic performance for HCC (**Figure 13H**). Additionally, the modulatory effect of miR-139-3p on HOXD-AS1 and DTNB expression was verified via qRT-PCR in three HCC cell lines, and the results revealed that the upregulation of miR-139-3p drastically reduced the expression levels of HOXD-AS1 and DTNB (**Figure 13I**, **13J**).

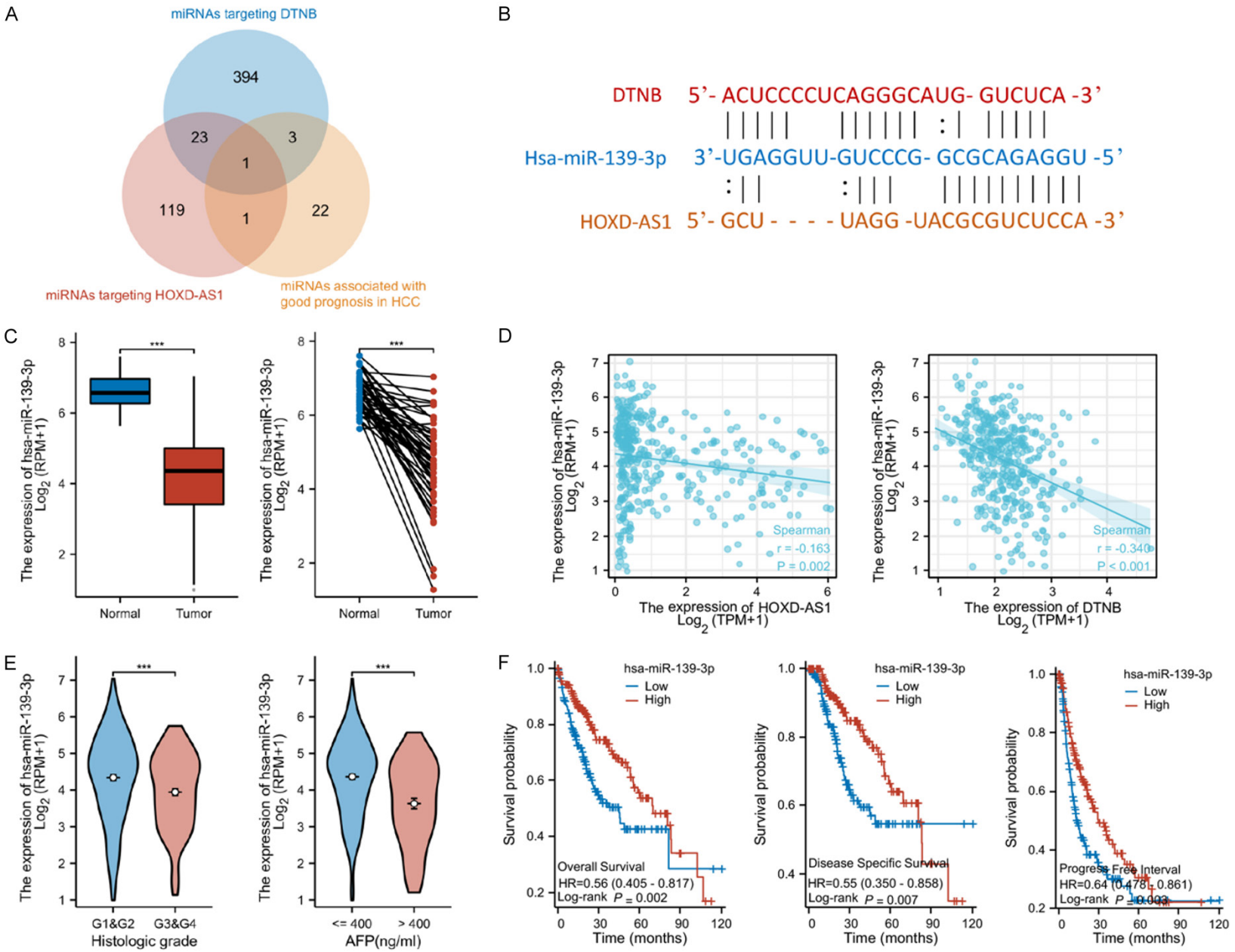
A
miRNAs targeting DTNB
394
23
3
1
119
1
22
miRNAs targeting HOXD-AS1
miRNAs associated with good prognosis in HCC
B
DTNB 5'- ACUCCCCUCAGGGCAUG- GUCUCA -3'
Hsa-miR-139-3p 3'-UGAGGUU-GUCCCG- GCGCAGAGGU -5'
HOXD-AS1 5'- GCU - - - - UAGG -UACGCGUCUCCA -3'
C
The expression of hsa-miR-139-3p Log2 (RPM+1)
***
Normal
Tumor
D
The expression of hsa-miR-139-3p Log2 (RPM+1)
Spearman
r = -0.163
P = 0.002
The expression of HOXD-AS1 Log2 (TPM+1)
Spearman
r = -0.340
P < 0.001
The expression of DTNB Log2 (TPM+1)
E
The expression of hsa-miR-139-3p Log2 (RPM+1)
G1&G2
G3&G4
Histologic grade
<= 400
> 400
AFP(ng/ml)
F
Survival probability
hsa-miR-139-3p
Low
High
Overall Survival
HR=0.56 (0.405 - 0.817)
Log-rank P = 0.002
Disease Specific Survival
HR=0.55 (0.350 - 0.858)
Log-rank P = 0.007
Progress Free Interval
HR=0.64 (0.478 - 0.861)
Log-rank P = 0.003
Time (months)

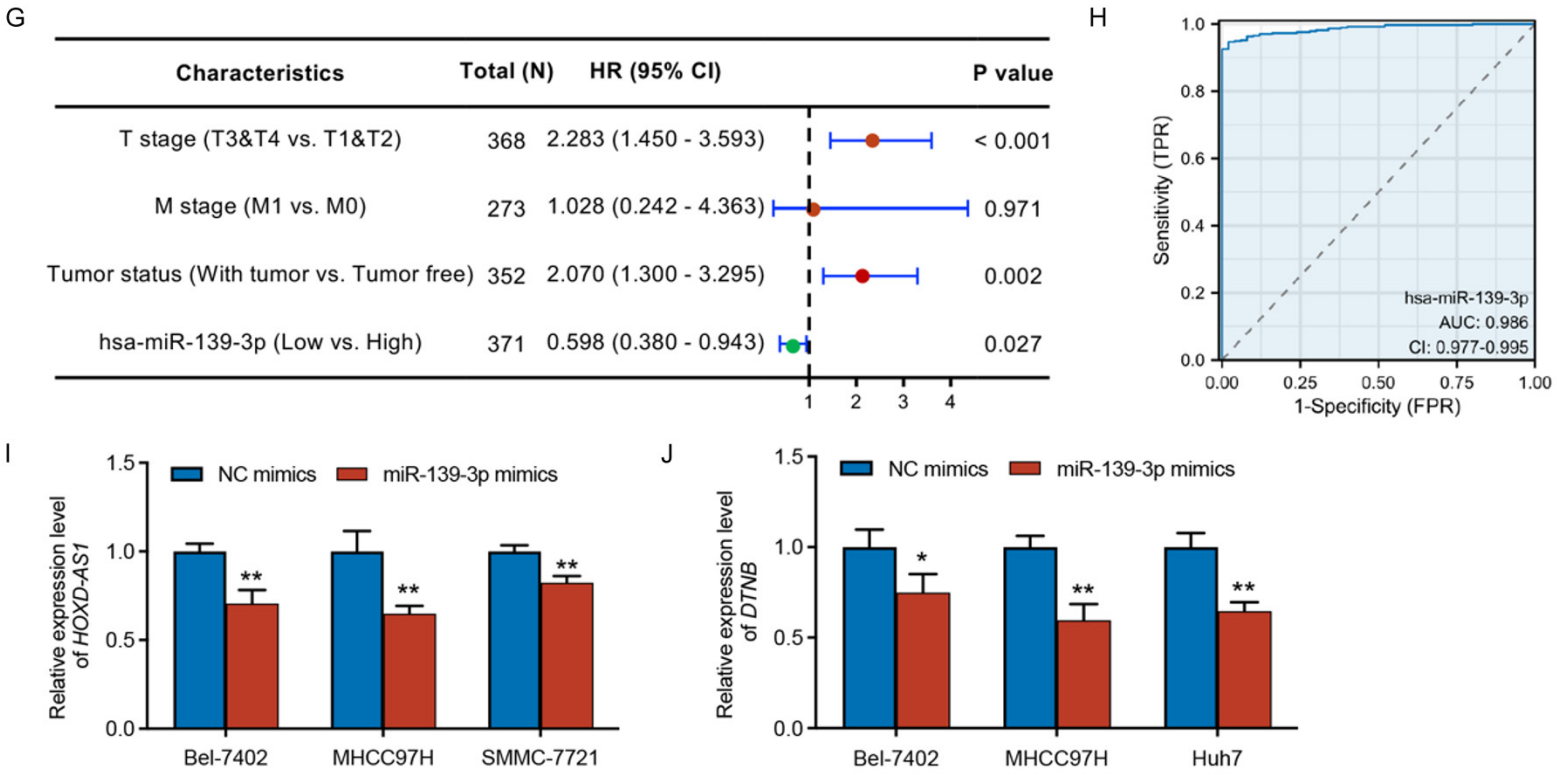

Figure 13. Identification of a potential ceRNA regulatory axis of HOXD-AS1/miR-139-3p/DTNB in HCC. (A) miR-139-3p was screened out by intersection of miRNAs that target both HOXD-AS1 and DTNB and miRNAs that are inversely correlated with poor prognosis of HCC patients. (B) Schematic representation of the putative miR-139-3p binding sites in HOXD-AS1 and DTNB. (C) The expression level of miR-139-3p in unpaired and paired HCC tissues were analysed using the TCGA data. (D) The correlation of miR-139-3p expression with HOXD-AS1 and DTNB in HCC was evaluated based on the TCGA data. (E) Elevated miR-139-3p was correlated with histological grade and the AFP level in HCC patients. (F) High miR-139-3p expression was correlated with good prognosis of HCC patients. (G) Forest plot showing results of multivariate Cox regression analysis of miR-139-3p expression for overall survival. (H) Diagnostic ROC curves of the miR-139-3p level in HCC. Effect of overexpression of miR-139-3p on the expression of HOXD-AS1 (I) and DTNB (J) in HCC cells. **P* < 0.05, ***P* < 0.01, ****P* < 0.001. AFP, alpha-fetoprotein; AUC, area under the curve; CI, confidence interval; FPR, false-positive rate; TPR, true-positive rate.

Experimental validation of the expression status of DTNB and its biological functions in HCC

The expression trends of DTNB were verified via qRT-PCR utilizing 25 pairs of HCC and corresponding nearby tissues, and the results revealed that the expression levels of DTNB in tumour tissue were markedly greater than those in nearby tissues (**Figure 14A**), which aligns with the above bioinformatics analysis results.

To clarify the biological roles of DTNB in HCC, Bel-7402 and MHCC97H cells, which highly express DTNB, were used for loss-of-function experiments (**Figure 1B**). As depicted in **Figure 14B** and **14C**, DTNB could be effectively suppressed at the mRNA and protein levels in both the Bel-7402 and MHCC97H cell lines by transfection with 50 nm siRNA. *In vitro* experiments revealed that the proliferation, colony formation, migration, and invasion of HCC cells were significantly inhibited after DTNB was silenced (**Figure 14D-G**), indicating that DTNB promotes HCC progression. Additionally, cell cycle analysis disclosed that DTNB knockdown arrested HCC cells at the G0/G1 phase (**Figure 14H**).

Discussion

HCC, a frequently occurring malignancy with significant morbidity and mortality rates, faces suboptimal clinical diagnosis and treatment outcomes because of the absence of efficient early detection techniques and treatment approaches for patients with intermediate to advanced HCC [21]. Consequently, the identification and development of novel molecular markers and therapeutic targets have emerged as a focal points in translational medicine research on HCC [22]. In recent years, the robust availability of public tumour-related data and the rapid development of bioinformatics mining technology have greatly accelerated the discovery of new tumour biomarkers and treatment targets.

DTNB, transcribed from the p23.3 region of human chromosome 2, was first discovered and identified as a dystrophin-related protein [8]. In previous studies, DTNB was shown to have different tissue expression patterns than other members of the small dystrophin family, i.e., DTNB is not expressed in muscle, but is abundantly expressed in non-muscle tissues such as the brain, kidney, liver and lung, suggesting that DTNB might have a distinct biological functions in development and disease [8]. Although DTNB has been demonstrated to play critical roles in brain development because it can modulate neuronal differentiation through interactions with iBRAF, BRAF3, pancortin-2 and other key neurodevelopmental proteins [11, 23], the biological function of DTNB is still poorly understood.

HOXD-AS1, a well-known oncogenic lncRNA, has been shown to participate in tumour progression by modulating several oncogenes. In the case of HCC, SOX4, SLC27A4, and ARHGAP11A they were revealed to be positively regulated by HOXD-AS1 and act as downstream genes mediating the promotion effect of HOXD-AS1 on HCC metastasis [19, 20, 24]. In our previous study, the influence of HOXD-AS1 silencing on the gene expression profile of HCC cells was investigated using RNA-seq, and DTNB expression levels were found to be dramatically reduced by HOXD-AS1 silencing, implying that DTNB may contribute to HCC progression as a downstream gene of HOXD-AS1 [14]. Nonetheless, the link between DTNB and HCC is still ambiguous.

In the present study, the expression status of DTNB and its clinical significance, potential biological roles, and the underlying mechanism in HCC were systematically analysed through bioinformatic analysis and experimental validation. First, the positive regulatory relationship between lncRNA HOXD-AS1 and DTNB in HCC cells was validated, suggesting that DTNB can be modulated by lncRNA HOXD-AS1 at the transcriptional level and may act as a potential downstream gene of HOXD-AS1 to promote HCC progression.

Second, a high DTNB expression level was found to be positively related to T stage, histological grade, tumour status, adjacent hepatic tissue inflammation, and the AFP level in HCC patients, whereas it was negatively related to OS, DSS, and the PFI. Multivariate Cox regression test revealed that the DTNB expression level was independently associated with the OS of HCC patients. The ROC curve further uncovered that the DTNB expression level exhibited a favorable predictive impact on HCC, T1-T2 stage, histological grade G1-G2, tumour status, OS, DSS, and PFI, suggesting that the expres-

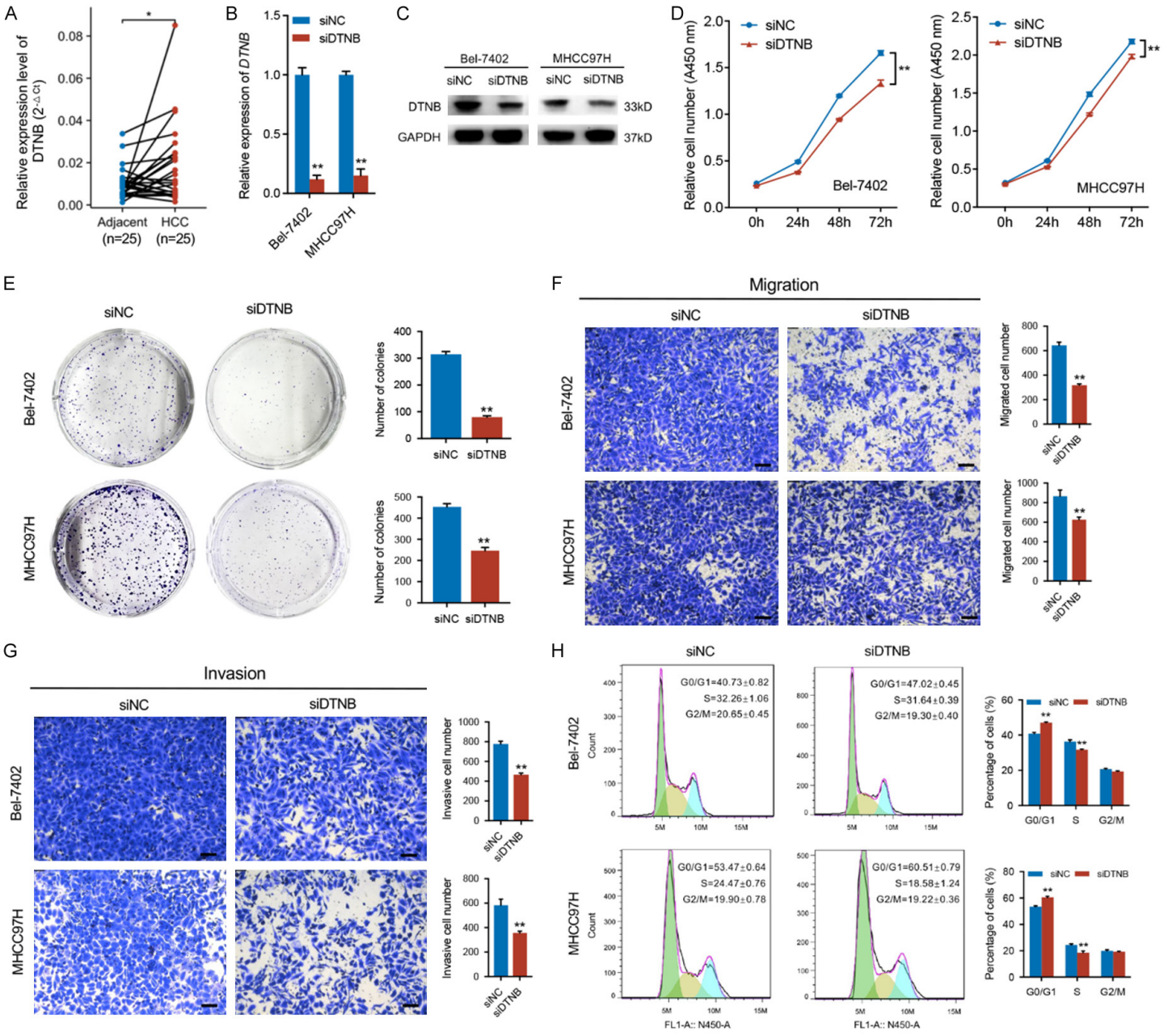
A
Relative expression level of DTNB (2^-Δct)
Adjacent (n=25)
HCC (n=25)
B
siNC
siDTNB
Relative expression of DTNB
Bel-7402
MHCC97H
C
Bel-7402
MHCC97H
siNC
siDTNB
DTNB
GAPDH
33kD
37kD
D
siNC
siDTNB
Relative cell number (A450 nm)
Bel-7402
MHCC97H
0h
24h
48h
72h
E
siNC
siDTNB
Bel-7402
MHCC97H
Number of colonies
F
Migration
Migrated cell number
G
Invasion
Invasive cell number
H
G0/G1=40.73±0.82
S=32.26±1.06
G2/M=20.65±0.45
G0/G1=47.02±0.45
S=31.64±0.39
G2/M=19.30±0.40
G0/G1=53.47±0.64
S=24.47±0.76
G2/M=19.90±0.78
G0/G1=60.51±0.79
S=18.58±1.24
G2/M=19.22±0.36
Count
FL1-A:: N450-A
Percentage of cells (%)
G0/G1
S
G2/M

Figure 14. Experimental validation of the expression status of DTNB and its biological roles in HCC. (A) The expression status of DTNB in 25 pairs of HCC and corresponding adjacent tissues were detected by qRT-PCR. The knockdown efficiency of DTNB in HCC cells was evaluated by qRT-PCR (B) and western blot (C). The effects of DTNB knockdown on the proliferative ability of HCC cells was detected by CCK-8 (D) and colony formation assay (E). The effects of DTNB knockdown on the migration (F) and invasion (G) of HCC cells were assessed by transwell assay. (H) The effect of DTNB knockdown on the cell cycle of HCC cells was examined via flow cytometry. $*P < 0.05$, $**P < 0.01$.

sion of DTNB could have utility as an innovative molecular indicator for the early detection and prognostication of HCC.

Third, the upregulation of DTNB was strongly linked to the infiltration of several immune cell types in HCC tissues. For example, the infiltration abundance of Th2 cells with tumour immunosuppressive functions was positively associated with DTNB expression levels in HCC tissues, whereas the infiltration abundance of pDCs, neutrophils, and Th17 cells with antitumour activity was negatively correlated with DTNB expression levels. The infiltration of Th2 cells into tumours can facilitate tumour growth or metastasis through the secretion of IL-4 and IL-10 to mediate immunosuppression [25, 26]. pDCs, as a specific group of dendritic cells, have the unique ability to excrete substantial amounts of type I INF-γ and were recently discovered to directly eliminate tumours by expressing tumour necrosis factor-related apoptosis-inducing ligand (TRAIL), secreting granzyme B, and increasing the antitumour capabilities of NK and T cells. Interestingly, the DTNB expression level was also positively related to the expression of multiple key immune checkpoint genes (also known as immunotherapeutic targets), such as PD-L1, PD-1, and CTLA4. In addition, the TIDE score of the low DTNB expression group was markedly lower than that of the high DTNB expression group, suggesting that HCC patients with lower DTNB expression levels may have greater sensitivity to immune checkpoint blockade therapy. Additionally, the DTNB expression was linked to the expression of most chemokines and receptor genes. Taken together, DTNB is closely involved in modulating the HCC tumour microenvironment and may be a potential immunotherapy target as well as a biomarker for predicting the effectiveness of immune checkpoint inhibitors in the treatment of HCC patients.

Fourth, the expression levels of DTNB in HCC were revealed to be related to the sensitivity to 17 anti-HCC drugs, suggesting that DTNB expression could serve as a possible biomarker to predict the therapeutic efficacy of these antitumour drugs and guide the personalized treatment of HCC patients. Notably, our research disclosed a positive correlation between DTNB expression and the IC50 values of cetuximab and erlotinib, indicating a low sensitivity to both cetuximab and erlotinib in HCC patients with elevated DTNB expression.

Fifth, the genes positively co-expressed with DTNB in HCC were identified, and the 10 hub genes (BUB1, CDK1, DLGAP5, KIF2C, CCNB1, BUB1B, CDC20, KIF11, KIF20A, and ASPM) were further picked out by constructing a PPI network. All these hub genes were found to be upregulated in HCC and positively related to the pathological T stage, histological grade, and poor OS of HCC patients. Functional prediction employing DTNB and its associated hub genes revealed that DTNB was closely related to the cell cycle. Furthermore, the possible biological roles and signaling pathways of DTNB in HCC were further predicted by performing the GSEA analysis using the differentially expressed genes between HCC patients with elevated and low DTNB expression, which revealed a strong positive correlation between the DTNB expression and the cell cycle, suggesting that DTNB might be involved in HCC progression through the modulation of cell proliferation. An earlier study demonstrated that DTNB could directly take part in the regulation of cell proliferation during the initial stage of neural differentiation of NT2/D1 cells [10], a pluripotent human embryonal carcinoma cell line used as a model of neural development [27]. However, the function of DTNB in the proliferation of tumour cells remains ambiguous.

Sixth, a potential ceRNA regulatory axis of HOXD-AS1/miR-139-3p/DTNB in HCC was identified. To date, several ceRNA pathways have been demonstrated to mediate the oncogenic role of HOXD-AS1 in HCC, such as HOXD-AS1/miR-130a-3p/SOX4 [19] and HOXD-AS1/miR-326/SLC27A4 [20]. Recently, miR-139-3p was revealed to sponge the oncogenic circular RNA (circRNA) to participate in HCC progres-

sion via a ceRNA mechanism. For example, circ_0003410 can facilitate the progression of HCC through increasing the proportion of M2/M1 macrophages via the miR-139-3p/CCL5 pathway [28]. Unfortunately, the miRNAs that regulate DTNB have not yet been identified. Therefore, this study was the first attempt to identify ceRNA regulatory mechanisms based on DTNB.

Finally, the expression status and biological roles of DTNB in HCC were validated by wet-lab experiments, which indicated that DTNB was overexpressed in HCC tissues and could accelerate the progression of HCC by affecting cell proliferation, migration, and invasion, thus confirming the findings obtained by bioinformatics analysis that DTNB was positively related to an unfavorable prognosis in patients with HCC. In addition, functional enrichment analysis suggested that DTNB is closely linked to the cell cycle, and the experimental validation results revealed that DTNB knockdown could result in the cell cycle arrest, thus verifying the prediction of the biological function of DTNB in HCC via bioinformatics.

Conclusions

The current study revealed that DTNB, a downstream target of the lncRNA HOXD-AS1, may have utility as a potential prognostic biomarker and therapeutic target in HCC, laying the groundwork for further basic and clinical translational research on DTNB in HCC.

Acknowledgements

This study was supported by the Natural Science Foundation Research Program of Shaanxi Province of China (2023-JC-YB-750, 2023-JC-YB-700 and 2024JC-YBMS-691), and the Science Research Foundation of the Second Affiliated Hospital of Xi'an Jiaotong University (2020YJ(ZYTS)546-09 and YJ(QN) 202014).

Disclosure of conflict of interest

None.

Address correspondence to: Jin Sun and Zongfang Li, National and Local Joint Engineering Research Center of Biodiagnostics and Biotherapy, The Second Affiliated Hospital, Xi'an Jiaotong University, No. 157 West 5th Road, Xi'an 710004, Shaanxi, China. E-mail: jinsun2014@xjtu.edu.cn (JS); lzf-2568@xjtu.edu.cn (ZFL)

References

[1] Brown ZJ, Tsilimigras DI, Ruff SM, Mohseni A, Kamel IR, Cloyd JM and Pawlik TM. Management of hepatocellular carcinoma: a review. JAMA Surg 2023; 158: 410-420.

[2] Singal AG, Kanwal F and Llovet JM. Global trends in hepatocellular carcinoma epidemiology: implications for screening, prevention and therapy. Nat Rev Clin Oncol 2023; 20: 864-884.

[3] Wang K, Wang R, Liu S, Peng G, Yu H and Wang X. Comparison of the safety and efficacy of hepatic resection and radiofrequency ablation in the treatment of single small hepatocellular carcinoma: systematic review and meta-analysis. Transl Cancer Res 2022; 11: 580-590.

[4] Nevola R, Ruocco R, Criscuolo L, Villani A, Alfano M, Beccia D, Imbriani S, Claar E, Cozzolino D, Sasso FC, Marrone A, Adinolfi LE and Rinaldi L. Predictors of early and late hepatocellular carcinoma recurrence. World J Gastroenterol 2023; 29: 1243-1260.

[5] Yang JC, Hu JJ, Li YX, Luo W, Liu JZ and Ye DW. Clinical applications of liquid biopsy in hepatocellular carcinoma. Front Oncol 2022; 12: 781820.

[6] Hagiwara S, Nishida N and Kudo M. Advances in immunotherapy for hepatocellular carcinoma. Cancers (Basel) 2023; 15: 2070.

[7] Wang Y and Deng B. Hepatocellular carcinoma: molecular mechanism, targeted therapy, and biomarkers. Cancer Metastasis Rev 2023; 42: 629-652.

[8] Blake DJ, Nawrotzki R, Loh NY, Gorecki DC and Davies KE. beta-dystrobrevin, a member of the dystrophin-related protein family. Proc Natl Acad Sci U S A 1998; 95: 241-246.

[9] Ceccarini M, Grasso M, Veroni C, Gambara G, Artegiani B, Macchia G, Ramoni C, Torreri P, Mallozzi C, Petrucci TC and Macioce P. Association of dystrobrevin and regulatory subunit of protein kinase A: a new role for dystrobrevin as a scaffold for signaling proteins. J Mol Biol 2007; 371: 1174-1187.

[10] Quaranta MT, Spinello I, Paolillo R, Macchia G, Boe A, Ceccarini M, Labbaye C and Macioce P. Identification of beta-dystrobrevin as a direct target of miR-143: involvement in early stages of neural differentiation. PLoS One 2016; 11: e0156325.

[11] Artegiani B, Labbaye C, Sferra A, Quaranta MT, Torreri P, Macchia G, Ceccarini M, Petrucci TC and Macioce P. The interaction with HMG20a/b proteins suggests a potential role for beta-dys-

trobrevin in neuronal differentiation. J Biol Chem 2010; 285: 24740-24750.
[12] Borutinskaite VV, Magnusson KE and Navakauskiene R. Histone deacetylase inhibitor BML-210 induces growth inhibition and apoptosis and regulates HDAC and DAPC complex expression levels in cervical cancer cells. Mol Biol Rep 2012; 39: 10179-10186.
[13] Li L, Wang Y, Zhang X, Huang Q, Diao Y, Yin H and Liu H. Long non-coding RNA HOXD-AS1 in cancer. Clin Chim Acta 2018; 487: 197-201.
[14] Sun J, Guo Y, Bie B, Zhu M, Tian H, Tian J, Li J, Yang Y, Ji F, Kong G and Li Z. Silencing of long noncoding RNA HOXD-AS1 inhibits proliferation, cell cycle progression, migration and invasion of hepatocellular carcinoma cells through MEK/ERK pathway. J Cell Biochem 2020; 121: 443-457.
[15] Hanzelmann S, Castelo R and Guinney J. GSVA: gene set variation analysis for microarray and RNA-seq data. BMC Bioinformatics 2013; 14: 7.
[16] Jiang P, Gu S, Pan D, Fu J, Sahu A, Hu X, Li Z, Traugh N, Bu X, Li B, Liu J, Freeman GJ, Brown MA, Wucherpfennig KW and Liu XS. Signatures of T cell dysfunction and exclusion predict cancer immunotherapy response. Nat Med 2018; 24: 1550-1558.
[17] Yang W, Soares J, Greninger P, Edelman EJ, Lightfoot H, Forbes S, Bindal N, Beare D, Smith JA, Thompson IR, Ramaswamy S, Futreal PA, Haber DA, Stratton MR, Benes C, McDermott U and Garnett MJ. Genomics of drug sensitivity in cancer (GDSC): a resource for therapeutic biomarker discovery in cancer cells. Nucleic Acids Res 2013; 41: D955-D961.
[18] Liu CJ, Hu FF, Xie GY, Miao YR, Li XW, Zeng Y and Guo AY. GSCA: an integrated platform for gene set cancer analysis at genomic, pharmacogenomic and immunogenomic levels. Brief Bioinform 2023; 24: bbac558.
[19] Wang H, Huo X, Yang XR, He J, Cheng L, Wang N, Deng X, Jin H, Wang N, Wang C, Zhao F, Fang J, Yao M, Fan J and Qin W. STAT3-mediated upregulation of lncRNA HOXD-AS1 as a ceRNA facilitates liver cancer metastasis by regulating SOX4. Mol Cancer 2017; 16: 136.
[20] Ji W, Wang Q and Yang J. LncRNA HOXD-AS1 promotes the metastasis of human hepatocellular carcinoma via modulating miR-326/SLC27A4. Cancer Cell Int 2020; 20: 161.
[21] Llovet JM, Kelley RK, Villanueva A, Singal AG, Pikarsky E, Roayaie S, Lencioni R, Koike K, Zucman-Rossi J and Finn RS. Hepatocellular carcinoma. Nat Rev Dis Primers 2021; 7: 6.
[22] El-Nakeep S. Molecular and genetic markers in hepatocellular carcinoma: in silico analysis to clinical validation (current limitations and future promises). World J Gastrointest Pathophysiol 2022; 13: 1-14.
[23] Veroni C, Grasso M, Macchia G, Ramoni C, Ceccarini M, Petrucci TC and Macioce P. beta-dystrobrevin, a kinesin-binding receptor, interacts with the extracellular matrix components pancortins. J Neurosci Res 2007; 85: 2631-2639.
[24] Lu S, Zhou J, Sun Y, Li N, Miao M, Jiao B and Chen H. The noncoding RNA HOXD-AS1 is a critical regulator of the metastasis and apoptosis phenotype in human hepatocellular carcinoma. Mol Cancer 2017; 16: 125.
[25] Mantovani A, Allavena P, Sica A and Balkwill F. Cancer-related inflammation. Nature 2008; 454: 436-444.
[26] Lee HL, Jang JW, Lee SW, Yoo SH, Kwon JH, Nam SW, Bae SH, Choi JY, Han NI and Yoon SK. Inflammatory cytokines and change of Th1/Th2 balance as prognostic indicators for hepatocellular carcinoma in patients treated with transarterial chemoembolization. Sci Rep 2019; 9: 3260.
[27] Pleasure SJ, Page C and Lee VM. Pure, postmitotic, polarized human neurons derived from NTera 2 cells provide a system for expressing exogenous proteins in terminally differentiated neurons. J Neurosci 1992; 12: 1802-1815.
[28] Cao P, Ma B, Sun D, Zhang W, Qiu J, Qin L and Xue X. hsa_circ_0003410 promotes hepatocellular carcinoma progression by increasing the ratio of M2/M1 macrophages through the miR-139-3p/CCL5 axis. Cancer Sci 2022; 113: 634-647.